

Probing non-orthogonality of eigenvectors in non-Hermitian matrix models: diagrammatic approach

Maciej A. Nowak^{* 1} and Wojciech Tarnowski^{†1}

¹M. Smoluchowski Institute of Physics and Mark Kac Complex Systems Research Center, Jagiellonian University, S. Łojasiewicza 11, PL 30-348 Kraków, Poland.

April 9, 2022

Abstract

Using large N arguments, we propose a scheme for calculations of the two-point eigenvector correlation function for non-normal random matrices in the large N limit. The setting generalizes the quaternionic extension of free probability to two-point functions. In the particular case of biunitarily invariant random matrices, we obtain a simple, general expression for the two-point eigenvector correlation function, which can be viewed as a further generalization of the single ring theorem. This construction has some striking similarities to the freeness of the second kind known for the Hermitian ensembles in large N . On the basis of several solved examples, we conjecture two kinds of microscopic universality of the eigenvectors - one in the bulk, and one at the rim. The form of the conjectured bulk universality agrees with the scaling limit found by Chalker and Mehlig [JT Chalker, B Mehlig, PRL, **81**, 3367 (1998)] in the case of the complex Ginibre ensemble.

1 Introduction

Non-normal operators are ubiquitous in physical models. Examples include hydrodynamics, open quantum systems, PT-symmetric Hamiltonians, Dirac operators in the presence of chemical potential or finite θ angle. Non-normality is responsible for the transient dynamics, sensitivity of the spectrum to perturbations, pseudoresonant behavior and rapid growth of the perturbations of the system [1]. These effects are relevant in plasma physics [2], fluid mechanics [3], ecology [4, 5], laser physics [6], atmospheric science [7], magnetohydrodynamics [8], just to mention a few. Non-normality is common in dynamical systems as its the simplest source is the asymmetry of coupling between components.

Historically, most of the studied properties of non-normal random operators dealt with the eigenvalues. The eigenvalues of such operators are usually complex-valued, and that called for the need of new calculational techniques, both at the level of macroscopic and microscopic correlations. Surprisingly, this quest for complex eigenvalues has shadowed the study of eigenvectors, which are perhaps most distinctive features of non-normal operators. In particular, non-normal operators have two sets of eigenvectors, left and right, which are non-orthogonal among themselves, but can be chosen to be bi-orthogonal, provided that non-normal operator can be diagonalized at all.

One of the first attempts to systematic understanding of the non-orthogonality of eigenvectors in non-Hermitian random matrices was made by Chalker and Mehlig [9, 10]. Despite their study concentrated on the complex Ginibre ensemble, perhaps the simplest non-normal random operator, the results turned out quite non-trivial and revealed the possibilities of well-hidden universal properties of eigenvectors of non-normal operators. Another connection of the properties of non-normal operators and their eigenvectors to free probability was established soon later [11], but the systematic study of this topic was not followed. Only very recently, the topic of eigenvectors of non-normal operators got the new boost. First, the transient growth driven by eigenvector non-orthogonality was proposed as a mechanism of amplification of neural signals in balanced neural networks [12, 13, 14] and giant amplification of noise crucial in the formation of Turing patterns [15, 16, 17]. Second, the non-orthogonality of eigenfunction was related to the statistics of resonance width shifts in open quantum systems [18], which was soon confirmed experimentally [19]. Third, the essential role of eigenvectors in stochastic motion of eigenvalues was revealed [20, 21, 22]. Last but not least, the topic has triggered the attention of the mathematical community [23, 24].

^{*}maciej.a.nowak@uj.edu.pl

[†]wojciech.tarnowski@uj.edu.pl

In this work we focus on statistical ensembles of complex non-Hermitian matrix models, the probability density of which is invariant under the action of the unitary group $P(X) = P(U X U^\dagger)$. We also assume that in the $N \rightarrow \infty$ limit, at which we are working, the eigenvalues of X concentrate on a compact domain of a complex plane. Our results are valid for $|z - w|$ of order 1. We will study one-point and two-point Green functions built out of left and right eigenvectors. Here we recall, that, If a non-normal matrix X can be diagonalized by a similarity transformation $X = S \Lambda S^{-1}$, it possesses two eigenvectors for each eigenvalue λ_i : right $|R_i\rangle$ (a column in the matrix notation) and left $\langle L_i|$ (row), satisfying the eigenequations

$$X |R_i\rangle = \lambda_i |R_i\rangle, \quad \langle L_i| X = \langle L_i| \lambda_i. \quad (1)$$

These eigenvectors are not orthogonal $\langle L_i|L_j\rangle \neq \delta_{ij} \neq \langle R_i|R_j\rangle$, but normalized by the biorthogonality condition $\langle L_i|R_j\rangle = \delta_{ij}$. They also satisfy the completeness relation $\sum_{k=1}^N |R_k\rangle \langle L_k| = \mathbf{1}$. These two properties leave a freedom of rescaling each eigenvector by a non-zero complex number, $|R_i\rangle \rightarrow c_i |R_i\rangle$ with $\langle L_i| \rightarrow \langle L_i| c_i^{-1}$. They also allow for multiplication by a unitary matrix $|R_i\rangle \rightarrow U |R_i\rangle$ and $\langle L_i| \rightarrow \langle L_i| U^\dagger$. Upon the second transformation the new vectors are not the eigenvectors of the original matrix but of a one given by the adjoint action of the unitary group $X \rightarrow UXU^\dagger$, which suggests that a natural probability measure should assign these two matrices equal probability density function (pdf). The simplest object invariant under these transformations is the matrix of overlaps $O_{ij} = \langle L_i|L_j\rangle \langle R_j|R_i\rangle$ [9, 10].

To see how the eigenvector correlation functions appear naturally, let us consider an average $\langle \frac{1}{N} \text{Tr} f(X)g(X^\dagger) \rangle$, where f, g are two functions analytic in the spectrum of X and $\langle f(X) \rangle = \int f(X)P(X)dX$ denotes the average with respect to pdf $P(X)$. Taking $f = g$, we get the (normalized) Frobenius norm of a function of a matrix. The $1/N$ normalization was taken to get a finite quantity in the $N \rightarrow \infty$ limit. Using the spectral decomposition $X = \sum_{k=1}^N |R_k\rangle \lambda_k \langle L_k|$ and inserting the identity, $1 = \int d\mu(z)\delta^{(2)}(z - \lambda_k)$ twice, we obtain the expression

$$\left\langle \frac{1}{N} \text{Tr} f(X)g(X^\dagger) \right\rangle = \int d\mu(z)d\mu(w)f(z)g(\bar{w})D(z, w), \quad (2)$$

with

$$D(z, w) = \left\langle \frac{1}{N} \sum_{k,l=1}^N O_{kl} \delta^{(2)}(z - \lambda_k) \delta^{(2)}(w - \lambda_l) \right\rangle. \quad (3)$$

The two dimensional Dirac delta is understood as two deltas for real and imaginary parts $\delta^{(2)}(z) = \delta(\text{Re}z)\delta(\text{Im}z)$, and the measure $d\mu(z) = dx dy$ for $z = x + iy$. $D(z, w)$ introduced in [9, 10] is the density of eigenvalues weighted by the invariant overlap of the corresponding eigenvectors. It is split into a regular and singular part $D(z, w) = \tilde{O}_1(z)\delta^{(2)}(z - w) + O_2(z, w)$, where

$$\tilde{O}_1(z) = \left\langle \frac{1}{N} \sum_{k=1}^N O_{kk} \delta^{(2)}(z - \lambda_k) \right\rangle, \quad O_2(z, w) = \left\langle \frac{1}{N} \sum_{\substack{k,l=1 \\ k \neq l}}^N O_{kl} \delta^{(2)}(z - \lambda_k) \delta^{(2)}(w - \lambda_l) \right\rangle. \quad (4)$$

So defined one-point function in the bulk and far from the rims of the complex spectra grows linearly with the size of a matrix. To have a finite limit in large N , one considers scaled function $O_1(z) = \frac{1}{N} \tilde{O}_1(z)$. Throughout the paper we shall use only the 'untilded' function.

The one-point function O_1 plays an important role in scattering in open chaotic cavities [25, 18] and random lasing [26, 27], where the so-called Petermann factor [28] modifies the quantum-limited linewidth of a laser. It is also crucial in the description of the diffusion processes on matrices [21, 22] and gives the expectation of the squared eigenvalue condition number [29], an important quantity governing the stability of eigenvalues [1, 30]. The exact calculations are possible for Gaussian matrices [9, 10, 23], in the matrix model for open chaotic scattering [26, 27, 31] and for products of small Gaussian matrices [32]. For the Ginibre matrix the full distribution of the diagonal overlap is available and turns out to be heavy-tailed, as discovered by Bourgade and Dubach [24] with the use of probabilistic techniques, and investigated later using integrable structure and supersymmetry by Fyodorov [33].

The two-point function is much less known. The exact results are obtained only for the Ginibre matrix [9, 10, 24] and for open chaotic scattering with a single channel coupling [31]. Even the asymptotic results are known only for Gaussian matrices [9, 10] and quantum scattering ensemble [34]. The aim of this paper is to extend the known asymptotic results and develop a diagrammatic technique for calculation of the two-point function in the large N limit.

The paper is organized as follows. In Section 2, to show an analogy between the formalism developer in this paper and the diagrammatic approach to one-point functions in non-Hermitian ensembles, we briefly recall the cornerstones of diagrammatic calculus [11] for one-point Green's functions in the large non-Hermitian ensembles. This encapsulates both the mean spectral density and the one-point eigenvector correlation function O_1 . An appendix A shows concrete calculations within this formalism for the Elliptic ensemble.

Section 3 contains the main body of the paper – a formalism for calculation of O_2 . We extend the diagrammatic technique introduced by Chalker and Mehlig for Gaussian matrices to any probability distribution with unitary symmetry. Regularizing and linearizing the product of resolvents, we embed them into the quaternionic space. An analysis of planar Feynman diagrams leads us to the matrix Bethe-Salpeter equation (45), which relates the product of resolvents with the one-point Green’s function and planar cumulants. The latter are encoded in their generating function – quaternionic R -transform, see (46). We also study the traced product of resolvents $\mathfrak{h}(z, \bar{w}) = \left\langle \frac{1}{N} \text{Tr}(z\mathbf{1} - X)^{-1}(\bar{w}\mathbf{1} - X^\dagger)^{-1} \right\rangle$, which allows for calculation of the average (2) as a Dunford-Taylor integral [35, 36]

$$\left\langle \frac{1}{N} \text{Tr}f(X)g(X^\dagger) \right\rangle = \frac{1}{(2\pi i)^2} \int_{\gamma} dz \int_{\bar{\gamma}} d\bar{w} f(z)g(\bar{w})\mathfrak{h}(z, \bar{w}), \quad (5)$$

where contours $\bar{\gamma}, \gamma$ encircle all eigenvalues of X clockwise and counterclockwise, respectively. We derive the equation for \mathfrak{h} , expressing it in terms of quaternionic R -transform and traced resolvents, see (48) and (49). We also analyze an important class of ensembles with biunitarily invariant pdf. We obtain a compact formula for the two-point eigenvector correlation function

$$O_2(z_1, z_2) = \frac{1}{\pi} \partial_{\bar{z}_1} \partial_{z_2} \frac{\bar{z}_1(z_1 - z_2)O_1(r_1) + z_2(\bar{z}_1 - \bar{z}_2)O_1(r_2)}{|z_1 - z_2|^2 [F(r_1) - F(r_2)]}, \quad (6)$$

where F is the radial cumulative distribution function (cdf), defined as $F(r) = 2\pi \int_0^r \rho(s) s ds$, with $\rho(s)$ the spectral density circularly symmetric on the complex plane. The one-point eigenvector function is related to F via [29]

$$O_1(r) = \frac{F(r)(1 - F(r))}{\pi r^2}, \quad (7)$$

and $r = |z|$. The traced product of resolvents is shown to take a universal form

$$\mathfrak{h}(z, \bar{w}) = \frac{1}{z\bar{w} - r_{out}^2}, \quad (8)$$

where r_{out} is the spectral radius. This result has been already obtained for the Ginibre ensemble [10] and, recently, for matrices with independent identically distributed (iid) entries [37].

Applications of the developed formalism are presented in Sec. 4, where we consider an elliptic ensemble, some exemplary matrices from the biunitarily invariant class: truncated unitary, induced Ginibre, product of two Ginibres and their ratio. As the last example we consider a pseudohermitian matrix – a product of two shifted GUE matrices. In Section 5, we discuss the consequences of our large N results on the microscopic regime. We conjecture, on the basis of few examples solved in the literature and using our own results, that the two-point eigenvector correlation functions may exhibit universal scaling, alike it happens for the microscopic spectral two-pointers in Hermitian matrix models. Section 6 concludes the paper and points at some possible further developments.

2 Non-Hermitian random matrices

In non-Hermitian random matrix theory one is primarily interested in the distribution of the eigenvalues $\rho(z) = \left\langle \frac{1}{N} \sum_{i=1}^N \delta^{(2)}(z - \lambda_i) \right\rangle$. The 2-dimensional Dirac delta can be recovered using the relation $\partial_{\bar{z}} \frac{1}{z} = \pi \delta^{(2)}(z)$. Unfortunately, the average over the ensemble of a trace of the resolvent $\mathfrak{g}(z) = \left\langle \frac{1}{N} \text{Tr}(z\mathbf{1} - X)^{-1} \right\rangle$ does not yield the correct result inside the spectrum, as one would naively expect. The reason for this failure is that differentiation and taking the ensemble average are not interchangeable. This phenomenon was coined as spontaneous breaking of holomorphic symmetry [38].

A way to circumvent this obstacle is to consider a regularization of the Dirac delta. In RMT one mostly considers 2D Poisson kernel

$$\pi \delta^{(2)}(z) = \lim_{\epsilon \rightarrow 0} \frac{\epsilon^2}{(|z|^2 + \epsilon^2)^2} = \lim_{\epsilon \rightarrow 0} \partial_{\bar{z}} \frac{\bar{z}}{|z|^2 + \epsilon^2}. \quad (9)$$

The expression on the right hand side provides a prescription how the resolvent in the spectrum of X should be regularized. Having this hint in mind, one defines

$$g(z, \bar{z}, w, \bar{w}) = \left\langle \frac{1}{N} \text{Tr}(\bar{z}\mathbf{1} - X^\dagger)[(z\mathbf{1} - X)(\bar{z}\mathbf{1} - X^\dagger) + |w|^2 \mathbf{1}]^{-1} \right\rangle. \quad (10)$$

The spectral density can be now calculated via

$$\rho(z, \bar{z}) = \frac{1}{\pi} \lim_{|w| \rightarrow 0} \partial_{\bar{z}} g(z, \bar{z}, w, \bar{w}), \quad (11)$$

which can be also understood as a Poisson law in 2D electrostatics, since

$$\rho(z, \bar{z}) = \lim_{|w| \rightarrow 0} \frac{1}{\pi} \partial_z \partial_{\bar{z}} \Phi(z, \bar{z}, w, \bar{w}), \quad (12)$$

where

$$\Phi(z, \bar{z}, w, \bar{w}) = \left\langle \frac{1}{N} \ln \det[(z\mathbf{1} - X)(\bar{z}\mathbf{1} - X^\dagger) + |w|^2 \mathbf{1}] \right\rangle \quad (13)$$

is the (regularized) electrostatic potential of charges interacting via repulsive central force $F(r) \sim \frac{1}{r}$.

2.1 Linearization

Due to the quadratic expression in X in the denominator, the average in (10) is intractable when non-normal matrices are considered. To circumvent this problem one introduces $2N \times 2N$ matrix [38, 39, 40, 41]

$$\mathcal{G} = \left\langle \begin{pmatrix} z\mathbf{1} - X & i\bar{w}\mathbf{1} \\ iw\mathbf{1} & \bar{z}\mathbf{1} - X^\dagger \end{pmatrix}^{-1} \right\rangle \quad (14)$$

and the block trace operation, mapping $2N \times 2N$ matrices onto 2×2 ones

$$\text{bTr} \begin{pmatrix} A & B \\ C & D \end{pmatrix} = \begin{pmatrix} \text{Tr}A & \text{Tr}B \\ \text{Tr}C & \text{Tr}D \end{pmatrix}. \quad (15)$$

Then, one defines the 2×2 Green's function

$$G(z, \bar{z}, w, \bar{w}) = \begin{pmatrix} G_{11} & G_{1\bar{1}} \\ G_{\bar{1}1} & G_{\bar{1}\bar{1}} \end{pmatrix} = \frac{1}{N} \text{bTr} \mathcal{G}(z, \bar{z}, w, \bar{w}). \quad (16)$$

Its upper-left entry is exactly the desired function g (cf. (10)). Once the Green's function is known, one gets four elements of G . The entry $G_{\bar{1}\bar{1}}$ is just the complex conjugate of G_{11} , thus does not provide any additional information. The off-diagonal entries $G_{1\bar{1}} = -\bar{G}_{\bar{1}1}$ in the large N limit give the one-point eigenvector correlation function [11]

$$O_1(z) = \lim_{|w| \rightarrow 0} -\frac{1}{\pi} G_{1\bar{1}} G_{\bar{1}1}. \quad (17)$$

2.2 Quaternionic structure

The Green's function can be conveniently written as

$$G = \left\langle \frac{1}{N} \text{bTr}(\mathcal{Q} - \mathcal{X})^{-1} \right\rangle = \begin{pmatrix} \partial_{Q_{11}} \Phi & \partial_{Q_{1\bar{1}}} \Phi \\ \partial_{Q_{\bar{1}1}} \Phi & \partial_{Q_{\bar{1}\bar{1}}} \Phi \end{pmatrix}. \quad (18)$$

with

$$\mathcal{X} = \begin{pmatrix} X & 0 \\ 0 & X^\dagger \end{pmatrix}, \quad \mathcal{Q} = Q \otimes \mathbf{1}, \quad Q = \begin{pmatrix} z & i\bar{w} \\ iw & \bar{z} \end{pmatrix}. \quad (19)$$

This form of the Green's function resembles its traditional form as a traced resolvent, but now its argument is a 2×2 matrix and the matrix X is duplicated to incorporate also X^\dagger . The matrix Q is a representation of a quaternion $q = x + iy + ju + kv$ with the identification $z = x + iy$ and $w = v + iu$ [42]. The entries of G satisfy the same algebraic constraints as Q , therefore G is itself a quaternion and we refer to it as the quaternionic Green's function, similarly \mathcal{G} is called the quaternionic resolvent.

2.3 Averages in large N

We are interested in calculations of the averages of some functions of X , e.g. $\langle f(X, X^\dagger) \rangle$, with respect to distributions invariant under the adjoint action of the unitary group $P(X) = P(U X U^\dagger)$. We parameterize them by

$$P(X) \sim \exp(-N \text{Tr} V(X, X^\dagger)). \quad (20)$$

$V(X, X^\dagger)$, often referred to as potential, has to be Hermitian and growing sufficiently fast at infinity. To simplify calculations, we split the potential into the Gaussian and the residual part. The Gaussian part can be conveniently parameterized with $\sigma > 0$ and $\tau \in [-1, 1]$ [43]

$$V_G(X, X^\dagger) = \frac{1}{\sigma^2(1 - \tau^2)} \left(X X^\dagger - \frac{\tau}{2} (X^2 + (X^\dagger)^2) \right). \quad (21)$$

Averages with respect to the Gaussian potential by the virtue of Wick's theorem reduce to products of pairwise expectations, called propagators

$$\langle X_{ab} X_{cd} \rangle_G = \frac{\sigma^2 \tau}{N} \delta_{ad} \delta_{bc}, \quad \langle X_{ab} X_{cd}^\dagger \rangle_G = \frac{\sigma^2}{N} \delta_{ad} \delta_{bc}. \quad (22)$$

The exponent of the residual part of the potential is expanded into series, which produces additional terms, called vertices, to be averaged with respect to the Gaussian distribution. To cope with the multitude of terms, we represent them as diagrams. This introduces a natural hierarchy of diagrams according to their scaling with the size of the matrix. The dominant contribution, which is of the order of 1, comes from planar diagrams. The subleading corrections can be classified by the genus of the surface at which they can be drawn without the intersection [44].

2.4 Moment expansion of the quaternionic resolvent

To calculate the average of the quaternionic resolvent, we expand it into a geometric series

$$\mathcal{G} = \mathcal{Q}^{-1} + \langle \mathcal{Q}^{-1} \mathcal{X} \mathcal{Q}^{-1} \rangle + \langle \mathcal{Q}^{-1} \mathcal{X} \mathcal{Q}^{-1} \mathcal{X} \mathcal{Q}^{-1} \rangle + \dots, \quad (23)$$

and perform averages in the large N , as described in the previous section. It is convenient to introduce a notation, which incorporates the block structure of the duplicated matrices. We therefore endow each matrix with two sets of indices, writing for example $\mathcal{G}_{\alpha\beta,ij}$. The first two Greek indices, which we also refer to as quaternionic indices, enumerate blocks and take values 1 and $\bar{1}$. The Latin ones, running from 1 to N enumerate matrices within each block. The space described by the Latin indices we call simply the matrix space. The block trace operation can be represented as a partial trace over the matrix space $G(z)_{\alpha\beta} = \frac{1}{N} \sum_{i=1}^N \mathcal{G}_{\alpha\beta,ii}$. Due to the fact, that the propagators are expressed in terms of Kronecker deltas, all averaged expressions have trivial matrix structure, e.g. $\mathcal{G} = G \otimes \mathbf{1}$, but we need this notation for the next section.

Among all diagrams contributing to \mathcal{G} we distinguish a class of one-line irreducible (1LI), i.e. the ones that cannot be split into two parts, connected only through \mathcal{Q}^{-1} . Let us denote as Σ a sum of all 1LI diagrams. This is a building block of the quaternionic resolvent, since any diagram can be decomposed into 1LI subdiagrams connected through \mathcal{Q}^{-1} . This gives a Schwinger-Dyson equation (here we restrict only to the quaternionic part)

$$G(Q) = Q^{-1} + Q^{-1} \Sigma(Q) Q^{-1} + Q^{-1} \Sigma(Q) Q^{-1} \Sigma(Q) Q^{-1} + \dots, \quad (24)$$

which can be written in a closed form

$$G(Q) = (Q - \Sigma(Q))^{-1}. \quad (25)$$

2.5 Quaternionic R-transform

To find G , one needs to relate Σ with G . To this end, let us consider diagrams contributing to averages of traced strings of X 's and X^\dagger 's such that all X 's and X^\dagger 's are connected with each other. A sum of them we call a cumulant (in field theory language it is known as a dressed vertex) and endow the respective average with a subscript c . We adopt a convenient notation for cumulants in which \dagger is associated with $\bar{1}$ index and, trivially, lack of conjugation with 1. We also encode the length of the string. An example reads

$$c_{\alpha_1 \alpha_2 \dots \alpha_k}^{(k)} = \left\langle \frac{1}{N} \text{Tr} X^{\alpha_1} X^{\alpha_2} \dots X^{\alpha_k} \right\rangle_c. \quad (26)$$

We also introduce the R -transform, which is a 2×2 matrix, defined through its expansion for small arguments

$$R_{\alpha\beta} = c_{\alpha}^{(1)} \delta_{\alpha\beta} + c_{\alpha\beta}^{(2)} Q_{\alpha\beta} + \sum_{\mu \in \{1, \bar{1}\}} c_{\alpha\mu\beta}^{(3)} Q_{\alpha\mu} Q_{\mu\beta} + \sum_{\mu, \nu \in \{1, \bar{1}\}} c_{\alpha\mu\nu\beta}^{(4)} Q_{\alpha\mu} Q_{\mu\nu} Q_{\nu\beta} + \dots \quad (27)$$

This definition written in terms of indices may not seem to be intuitive, but in the matrix notation takes a clearer form

$$R(Q) \otimes \mathbf{1} = \langle \mathcal{X} \rangle_c + \langle \mathcal{X} \mathcal{Q} \mathcal{X} \rangle_c + \langle \mathcal{X} \mathcal{Q} \mathcal{X} \mathcal{Q} \mathcal{X} \rangle_c + \dots, \quad (28)$$

which is the counterpart of (23). The matrix R is also a quaternion, so it is dubbed as the quaternionic R -transform. Q is always associated with two consecutive indices in the cumulant and can be thought of as a transfer matrix. It is crucial for encoding all cumulants in the R -transform that matrices \mathcal{X} and \mathcal{Q} do not commute.

Consider now any 1LI diagram. Due to its irreducibility it can be depicted as a certain cumulant connecting first and the last \mathcal{X} and possibly some others in between. The subdiagrams disconnected from the cumulant

can be in any form, which is already encoded in the quaternionic Green's function. This allows us to write the second Schwinger-Dyson equation relating Σ and G via the quaternionic R -transform

$$\Sigma(Q) = R(G(Q)). \quad (29)$$

The knowledge of all cumulants allows us to solve the matrix model, since equations (25) and (29) can be brought to a single 2×2 matrix equation

$$R(G(Q)) + G(Q)^{-1} = Q. \quad (30)$$

3 2-point eigenvector correlation function

3.1 Preliminaries

In order to investigate the 2-point eigenvector correlation function associated with the off-diagonal overlap, we follow the paradigm outlined in the previous section for calculations of the Green's function. A naive approach, i.e. calculation of $\mathfrak{h}(z_1, \bar{z}_2) = \left\langle \frac{1}{N} \text{Tr}(z_1 \mathbf{1} - X)^{-1} (\bar{z}_2 \mathbf{1} - X^\dagger)^{-1} \right\rangle$, yields the result which is correct only outside of the spectrum of X , which we refer to as the holomorphic solution. Inside the spectrum, we regularize each resolvent, using the rule

$$(z \mathbf{1} - X)^{-1} \rightarrow (\bar{z} \mathbf{1} - X^\dagger) M(z, w)^{-1}, \quad (31)$$

where $M(z, w) = (z \mathbf{1} - X)(\bar{z} \mathbf{1} - X^\dagger) + |w|^2 \mathbf{1}$. We shall therefore study

$$h(z_1, w_1, z_2, w_2) = \left\langle \frac{1}{N} \text{Tr}(\bar{z}_1 \mathbf{1} - X^\dagger) M(z_1, w_1)^{-1} M(z_2, w_2)^{-1} (z_2 \mathbf{1} - X) \right\rangle. \quad (32)$$

The weighted density is therefore given by

$$D(z_1, z_2) = \lim_{|w_1|, |w_2| \rightarrow 0} \frac{1}{\pi^2} \partial_{\bar{z}_1} \partial_{z_2} h(z_1, w_1, z_2, w_2). \quad (33)$$

In this paper we will calculate h by diagrammatic $1/N$ expansion in the planar limit. The singular part of $D(z_1, z_2)$ containing Dirac delta is not accessible in perturbative calculations, so we get

$$O_2(z_1, z_2) = \lim_{|w_1|, |w_2| \rightarrow 0} \frac{1}{\pi^2} \partial_{\bar{z}_1} \partial_{z_2} h(z_1, w_1, z_2, w_2). \quad (34)$$

There exists a class of matrices which despite not being Hermitian have real spectrum. A simple example is a product of two Hermitian matrices A, B , one of which, A , is positive definite. The resulting matrix is not Hermitian, but isospectral to $A^{1/2} B A^{1/2}$, which must have real eigenvalues. The eigenvectors of AB are not orthogonal, which makes O_2 not trivial. The reality of the spectrum facilitates calculations, as the knowledge of the traced resolvent is sufficient. Thanks to the Sokhocki-Plemelj formula valid for real x

$$2\pi i \delta(x) = \lim_{\epsilon \rightarrow 0} \left(\frac{1}{x - i\epsilon} - \frac{1}{x + i\epsilon} \right), \quad (35)$$

the two-point function can be calculated from the holomorphic function via

$$O_2(x, y) = \frac{-1}{4\pi^2} (\mathfrak{h}(+, +) - \mathfrak{h}(+, -) - \mathfrak{h}(-, +) + \mathfrak{h}(-, -)), \quad (36)$$

where

$$\mathfrak{h}(\pm, \pm) = \lim_{\epsilon_1, \epsilon_2 \rightarrow 0} \mathfrak{h}(x \pm i\epsilon_1, y \pm i\epsilon_2) \quad (37)$$

and signs are uncorrelated.

3.2 Linearization

The expression for the regularized product of resolvents (32) contains two quadratic nonlinearities. We overcome this difficulty, by using $2N \times 2N$ matrices $\mathcal{Q} = Q \otimes \mathbf{1}$, $\mathcal{P} = P \otimes \mathbf{1}$ and \mathcal{X} , where

$$Q = \begin{pmatrix} z_1 & i\bar{w}_1 \\ iw_1 & \bar{z}_1 \end{pmatrix}, \quad P = \begin{pmatrix} z_2 & i\bar{w}_2 \\ iw_2 & \bar{z}_2 \end{pmatrix}, \quad \mathcal{X} = \begin{pmatrix} X & 0 \\ 0 & X^\dagger \end{pmatrix}. \quad (38)$$

We define the average of the Kronecker product of two quaternionic resolvents

$$\mathcal{H} = \langle (\mathcal{Q} - \mathcal{X})^{-1} \otimes (\mathcal{P}^T - \mathcal{X}^T)^{-1} \rangle. \quad (39)$$

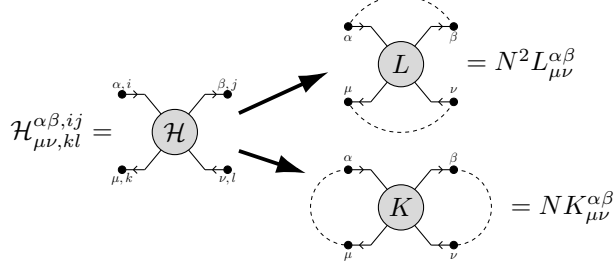


Figure 1: Possible contractions of matrix indices (dashed lines) of the Kronecker product of two quaternionic resolvents. The way how one contracts indices determines the class dominant planar diagrams, which are drawn between dashed lines and the horizontal baselines. The upper choice corresponds to a class of double-trace two-point functions, see (80), while the lower possibility leads a single-trace two point function encoding correlations of eigenvectors. Diagrams contributing to L are of wheel type [45, 46] and K is given as a sum of ladder diagrams.

Such an object is quite unusual in Random Matrix Theory. A similar construction was used by Brezin and Zee for calculation of the connected 2-point density in Hermitian models [45], but there one deals only with matrix indices. To the best of our knowledge the quaternionic approach to two-point functions for non-Hermitian matrices is considered for the first time, thus we will discuss it in more details.

\mathcal{H} is a $4N^2 \times 4N^2$ matrix with a very specific block structure. To keep track of it, we endow \mathcal{H} with 8 indices. The upper ones refer to the first matrix in the Kronecker product, while the lower ones to the second. As in the case of the quaternionic Green's function, Greek indices, taking values in $\{1, \bar{1}\}$, enumerate blocks, while Latin indices ranging in $\{1, \dots, N\}$ denote elements within each block. In the index notation, its components read (note the transpose of the second matrix)

$$\mathcal{H}_{\mu\nu,kl}^{\alpha\beta,ij} = \left\langle (\mathcal{Q} - \mathcal{X})_{\alpha\beta,ij}^{-1} (\mathcal{P} - \mathcal{X})_{\nu\mu,lk}^{-1} \right\rangle. \quad (40)$$

The resolvents are then expanded into power series

$$\mathcal{H} = \left\langle (\mathcal{Q}^{-1} + \mathcal{Q}^{-1}\mathcal{X}\mathcal{Q}^{-1} + \dots) \otimes (\mathcal{P}^{-1} + \mathcal{P}^{-1}\mathcal{X}\mathcal{P}^{-1} + \dots)^T \right\rangle, \quad (41)$$

and taking the expectation produces diagrams. The flow of Latin (matrix) indices in the diagrams follows the lines in the double line notation. The propagators are symmetric, thus the direction does not matter. The flow of quaternionic (Greek) indices is governed by their order in the expansion of the resolvent. Since the quaternion matrices Q and P are not symmetric, the direction matters and is depicted by an arrow. We draw diagrams in such a way that the terms in the expansion of the resolvents are in two rows, hereafter called baselines, with the first resolvent above. The quaternionic indices flow from left to right in the upper baseline and in the opposite direction below.

There are two ways of contracting matrix indices ¹, which preserves planarity of diagrams, thus we define two functions

$$K_{\mu\nu}^{\alpha\beta} = \frac{1}{N} \sum_{i,j=1}^N \mathcal{H}_{\mu\nu,ij}^{\alpha\beta,ii}, \quad L_{\mu\nu}^{\alpha\beta} = \frac{1}{N^2} \sum_{i,j=1}^N \mathcal{H}_{\mu\nu,ij}^{\alpha\beta,ij}, \quad (42)$$

which correspond to contractions presented in Fig. 1. These two possible contractions define two different classes of planar diagrams. The admissible diagrams have to be drawn in a region of a plane bounded by baselines and dashed lines depicting contractions. The diagrams contributing to K are of the ladder type, while the class of planar diagrams contributing to L , coined as wheel diagrams, is broader, as it admits for circumventing one of the baselines. In this section we concentrate on the ladder diagrams.

3.3 Ladder diagrams

In this section we are interested in calculation of K . The contraction of matrix indices in \mathcal{H} which leads to K is in fact a summation of all N^4 elements within each 4×4 block. To make the notation of Greek indices even more explicit, we write the entries of K

$$K = \begin{pmatrix} K_{11}^{11} & K_{11}^{1\bar{1}} & K_{1\bar{1}}^{1\bar{1}} & K_{1\bar{1}}^{1\bar{1}} \\ K_{11}^{\bar{1}\bar{1}} & K_{1\bar{1}}^{\bar{1}\bar{1}} & K_{\bar{1}\bar{1}}^{\bar{1}\bar{1}} & K_{\bar{1}\bar{1}}^{\bar{1}\bar{1}} \\ K_{1\bar{1}}^{1\bar{1}} & K_{1\bar{1}}^{1\bar{1}} & K_{1\bar{1}}^{1\bar{1}} & K_{1\bar{1}}^{1\bar{1}} \\ K_{\bar{1}\bar{1}}^{1\bar{1}} & K_{\bar{1}\bar{1}}^{1\bar{1}} & K_{\bar{1}\bar{1}}^{1\bar{1}} & K_{\bar{1}\bar{1}}^{1\bar{1}} \end{pmatrix} \quad (43)$$

¹In fact, there are $\frac{4!}{2^2 \cdot 2!} = 3$ ways, but $\mathcal{H}_{\mu\nu,ji}^{\alpha\beta,ij}$ leads to the same diagrams as $K_{\mu\nu}^{\beta\alpha}$

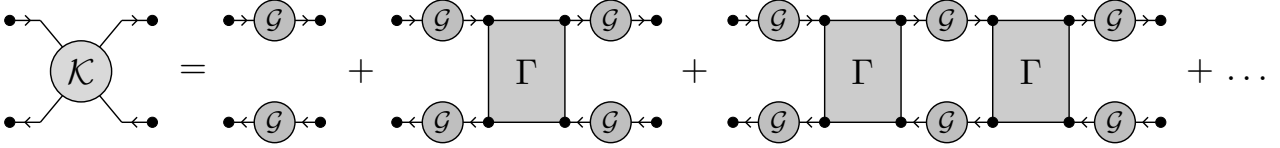


Figure 2: The general structure of planar ladder diagrams contributing to \mathcal{K} .

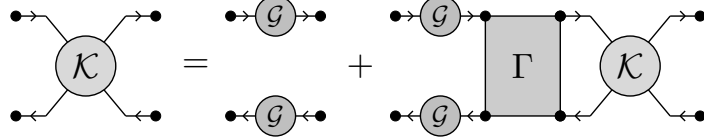


Figure 3: Matrix Bethe-Salpeter equation (44). In the planar limit $\Gamma_{\mu\nu,kl}^{\alpha\beta,ij} = \frac{1}{N} B_{\mu\nu}^{\alpha\beta} \delta_k^i \delta_l^j$, allowing for calculation of K .

An important consequence of this construction is that the K_{11}^{11} element is exactly the desired function h (32) for the calculation of the eigenvector correlation function.

Let us define $\mathcal{K}_{\mu\nu,kl}^{\alpha\beta,ij}$ a sum of all ladder diagrams contributing to K (before we contract indices). A vertex can connect two points on a baseline (a rail of the ladder), which results as dressing of the part of the rail. There are also vertices connecting two baselines, which give rise to the rungs of the ladder. If we denote $\Gamma_{\mu\nu,kl}^{\alpha\beta,ij}$ a sum of all connected subdiagrams which connect two rails, one can express \mathcal{K} in terms of Γ as a geometric series, presented in Fig. 2, which can be written in a closed form (a sum over repeating indices is implicit)

$$\mathcal{K}_{\mu\nu,cd}^{\alpha\beta,ab} = G^{\alpha\beta} G_{\mu\nu} \delta^{ab} \delta_{cd} + G^{\alpha\gamma} G_{\mu\rho} \delta^{ai} \delta_{cj} \Gamma_{\rho\sigma,jl}^{\gamma\epsilon,ik} \mathcal{K}_{\sigma\nu,ld}^{\epsilon\beta,kb}. \quad (44)$$

This relation, shown diagrammatically in Fig. 3, known as the matrix Bethe-Salpeter equation, is the counterpart of the Schwinger-Dyson equation for the two-point function, with Γ the counterpart of the self-energy.

A direct analysis of planar diagrams yields $\Gamma_{\mu\nu,kl}^{\alpha\beta,ij} = \frac{1}{N} B_{\mu\nu}^{\alpha\beta} \delta_k^i \delta_l^j$, where B is of order 1. Using the matrix structure of Γ , we trace out the matrix indices and find the equation for K , which in the matrix notation reads

$$K(Q, P) = G(Q) \otimes G^T(P) + [G(Q) \otimes G^T(P)] B(Q, P) K(Q, P). \quad (45)$$

We now turn our attention into the rungs. Any diagram contributing to Γ can be decomposed as a certain cumulant of length $n \geq 2$, the first k legs of which are attached to the upper rail, while the last legs are connected to the lower rail. The part of the rail between the legs of the cumulant gets dressed to the quaternionic Green's function $G(Q)$ above and $G(P)$ below. The space between k -th and $(k+1)$ -th legs is left unfilled, because the quaternionic indices at the end of rails are not contracted. This decomposition of Γ is depicted in Fig. 4. As Γ is completely determined by the planar cumulants, $B_{\mu\nu}^{\alpha\beta}$ can be calculated from the quaternionic R transform (27). The rule is simple and goes as follows.

Consider the expansion of $R_{\alpha\mu}$ in Q (27) and differentiate it with respect to $Q_{\beta\nu}$. As a result for some $0 < k < n-1$ the k -th quaternion $Q_{\mu_k \mu_{k+1}}$ will be replaced by $\delta_{\mu_k \beta} \delta_{\nu \mu_{k+1}}$. Then all $Q_{\mu_l \mu_{l+1}}$'s from the lhs of the removed Q (i.e. for $l < k$) are replaced by $G^{\mu_l \mu_{l+1}}(Q)$ and all $Q_{\mu_l \mu_{l+1}}$ on the right ($l > k$) by $G^{\mu_l \mu_{l+1}}(P)$. Then the sum over all possible positions (i.e. k 's), where Q has been removed, is performed.

B can be therefore expressed in terms of cumulants as a power series

$$B_{\mu\nu}^{\alpha\beta}(Q, P) = \sum_{k,l=1}^{\infty} \sum_{\substack{\sigma_1, \dots, \sigma_k \\ \rho_1, \dots, \rho_l}} \delta^{\alpha\sigma_1} \delta^{\beta\sigma_k} \delta_{\mu\rho_l} \delta_{\nu\rho_1} c_{\sigma_1 \dots \sigma_k \rho_1 \dots \rho_l}^{(k+l)} G^{\sigma_1 \sigma_2}(Q) \dots G^{\sigma_{k-1} \sigma_k}(Q) G_{\rho_1 \rho_2}(P) \dots G_{\rho_{l-1} \rho_l}(P), \quad (46)$$

where all σ_i and ρ_j take values in $\{1, \bar{1}\}$ and for $k=1$ or $l=1$ $G_{\sigma_k \sigma_{k+1}}$ reduces to Kronecker delta. An application of this procedure to the quantum scattering ensemble is presented in Appendix B.

We remark that the additivity of the quaternionic R -transform under the addition of unitarily invariant non-Hermitian matrices implies additivity of B .

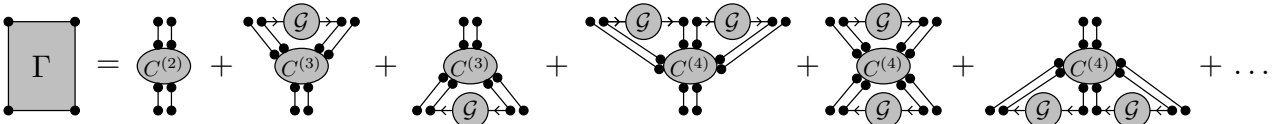


Figure 4: Γ given by the planar cumulants.

3.4 Traced product of resolvents

In the holomorphic domain outside the spectrum situation simplifies considerably, because one can set $|w| \rightarrow 0$ at the very beginning of calculations. The Green's function is then diagonal $G(z, \bar{z}) = \text{diag}(\mathbf{g}(z), \bar{\mathbf{g}}(\bar{z}))$, where $\mathbf{g}(z) = \langle \frac{1}{N} \text{Tr}(z\mathbf{1} - X)^{-1} \rangle$ and $\bar{\mathbf{g}}(\bar{z}) = \langle \frac{1}{N} \text{Tr}(\bar{z}\mathbf{1} - X^\dagger)^{-1} \rangle$. Due to such structure, B is also diagonal with components

$$B_{\mu\nu}^{\alpha\beta} = \delta^{\alpha\beta} \delta_{\mu\nu} \sum_{k,l=1}^{\infty} c_{\underbrace{\alpha \dots \alpha}_k \underbrace{\mu \dots \mu}_l}^{(k+l)} (\mathbf{g}_\alpha(z_1))^{k-1} (\mathbf{g}_\mu(z_2))^{l-1}, \quad (47)$$

where we assume a standard convention $\mathbf{g}_1(z) = \mathbf{g}(z)$ and $\mathbf{g}_{\bar{1}}(z) = \bar{\mathbf{g}}(\bar{z})$. A matrix equation (45) splits into decoupled scalar equations with the explicit solution for the component of our interest

$$K_{1\bar{1}}^{11} = \frac{\mathbf{g}(z_1)\bar{\mathbf{g}}(\bar{z}_2)}{1 - \mathbf{g}(z_1)\bar{\mathbf{g}}(\bar{z}_2)B_{1\bar{1}}^{11}}. \quad (48)$$

We read out the explicit form of the component of B from (47)

$$B_{1\bar{1}}^{11} = \sum_{k,l=1}^{\infty} c_{\underbrace{1 \dots 1}_k \underbrace{\bar{1} \dots \bar{1}}_l}^{(k+l)} (\mathbf{g}(z_1))^{k-1} (\bar{\mathbf{g}}(\bar{z}_2))^{l-1}, \quad (49)$$

Despite the fact that the mapping between cumulants and R -transform is not one to one [47], some cumulants can be uniquely determined from the knowledge of $R(Q)$. The cumulants $c_{\underbrace{1 \dots 1}_k \underbrace{\bar{1} \dots \bar{1}}_{n-k}}^{(n)}$ are the coefficients at $Q_{11}^{k-1} Q_{1\bar{1}} Q_{\bar{1}\bar{1}}^{n-k-1}$ in the expansion of $R_{1\bar{1}}(Q)$. One can easily see that there are no other cumulants contributing to this term.

All cumulants contributing to $R_{1\bar{1}}$ have at least one X^\dagger following X in the string, therefore $R_{1\bar{1}}$ is divisible by $Q_{1\bar{1}}$. Let us define $\tilde{R}_{1\bar{1}} = R_{1\bar{1}}/Q_{1\bar{1}}$, which is regular at 0. The considered cumulants are the only ones in which X is followed by X^\dagger exactly once. To exclude all other possibilities in the expansion of $\tilde{R}_{1\bar{1}}$, we set $Q_{1\bar{1}} = 0 = Q_{\bar{1}\bar{1}}$ in $\tilde{R}_{1\bar{1}}(Q)$. To reproduce (49) from $\tilde{R}_{1\bar{1}}$ one also needs to replace Q_{11} by $\mathbf{g}(z_1)$ and $Q_{\bar{1}\bar{1}}$ by $\bar{\mathbf{g}}(\bar{z}_2)$. Finally,

$$B_{1\bar{1}}^{11} = \tilde{R}_{1\bar{1}}(\text{diag}(\mathbf{g}(z_1), \bar{\mathbf{g}}(\bar{z}_2))). \quad (50)$$

3.5 Biunitarily invariant ensembles

In this subsection we consider a class of ensembles, the pdf of which is invariant under the multiplication by two unitary matrices, i.e. $P(X) = P(UXV^\dagger)$. In the large N the spectral density, which is rotationally invariant, is supported on either a disc or an annulus, a phenomenon coined as 'the single ring theorem' [48, 49]. The enhanced symmetry allows one to relate the distribution of eigenvalues and singular values both in the $N \rightarrow \infty$ limit [50] and for finite N [51]. More precisely, the radial cumulative distribution function $F(r) = 2\pi \int_0^r \rho(s) s ds$ is given by the solution of a simple functional equation $S_{XX^\dagger}(F(r) - 1) = \frac{1}{r^2}$, where S_{XX^\dagger} is the Voiculescu S -transform of the density of squared singular values [50]. Recently, this result was extended to the one-point eigenvector correlation function, which is determined solely by F [29, 47]

$$O_1(r) = \frac{F(r)(1 - F(r))}{\pi r^2}. \quad (51)$$

Such simple results in large N are possible because of exceptionally simple structure of cumulants. The only non-zero planar cumulants are the alternating ones [47], $\alpha_n = c_{1\bar{1} \dots 1\bar{1}}^{(2n)} = c_{\bar{1}\bar{1} \dots \bar{1}\bar{1}}^{(2n)}$. They can be encoded in a function of a single scalar variable $A(x) = \sum_{k=1}^{\infty} \alpha_n x^{n-1}$, called the determining sequence [52]. Due to this, only four components (out of 16) of B do not vanish. These are namely $B_{1\bar{1}}^{11} = B_{\bar{1}\bar{1}}^{11}$, $B_{1\bar{1}}^{1\bar{1}}$, $B_{\bar{1}\bar{1}}^{1\bar{1}}$.

A direct application of the formula (46) leads to

$$B_{1\bar{1}}^{11} = \sum_{k,l=1}^{\infty} \alpha_{k+l-1} [G_{1\bar{1}}(Q)G_{\bar{1}\bar{1}}(Q)]^{k-1} [G_{1\bar{1}}(P)G_{\bar{1}\bar{1}}(P)]^{l-1} \quad (52)$$

$$B_{1\bar{1}}^{1\bar{1}} = G_{1\bar{1}}(Q)G_{1\bar{1}}(P) \sum_{k,l=1}^{\infty} \alpha_{k+l} [G_{1\bar{1}}(Q)G_{\bar{1}\bar{1}}(Q)]^{k-1} [G_{1\bar{1}}(P)G_{\bar{1}\bar{1}}(P)]^{l-1} \quad (53)$$

$$B_{\bar{1}\bar{1}}^{1\bar{1}} = G_{\bar{1}\bar{1}}(Q)G_{\bar{1}\bar{1}}(P) \sum_{k,l=1}^{\infty} \alpha_{k+l} [G_{1\bar{1}}(Q)G_{\bar{1}\bar{1}}(Q)]^{k-1} [G_{1\bar{1}}(P)G_{\bar{1}\bar{1}}(P)]^{l-1} \quad (54)$$

The components of B can be expressed through auxiliary functions

$$B_{1\bar{1}}^{11} = B_{\bar{1}1}^{\bar{1}\bar{1}} = S(G_{1\bar{1}}(Q)G_{\bar{1}1}(Q), G_{1\bar{1}}(P)G_{\bar{1}1}(P)), \quad (55)$$

$$B_{1\bar{1}}^{1\bar{1}} = G_{1\bar{1}}(Q)G_{\bar{1}1}(P)T(G_{1\bar{1}}(Q)G_{\bar{1}1}(Q), G_{1\bar{1}}(P)G_{\bar{1}1}(P)), \quad (56)$$

$$B_{\bar{1}1}^{\bar{1}1} = G_{\bar{1}1}(Q)G_{1\bar{1}}(P)T(G_{1\bar{1}}(Q)G_{\bar{1}1}(Q), G_{1\bar{1}}(P)G_{\bar{1}1}(P)), \quad (57)$$

where

$$S(x, y) = \sum_{k,l=1}^{\infty} \alpha_{k+l-1} x^{k-1} y^{l-1} = \frac{x A(x) - y A(y)}{x - y}, \quad (58)$$

$$T(x, y) = \sum_{k,l=1}^{\infty} \alpha_{k+l} x^{k-1} y^{l-1} = \frac{A(x) - A(y)}{x - y}, \quad (59)$$

with A the determining sequence.

We remark that the average over the ensemble has been already taken at the level of Feynman diagrams and at this moment, we can safely remove the regularization. There are further simplifications for the biunitarily invariant matrices [47]

$$G_{1\bar{1}}G_{\bar{1}1}A(G_{1\bar{1}}G_{\bar{1}1}) = F(r) - 1, \quad G_{1\bar{1}}G_{\bar{1}1} = -\pi O_1(r). \quad (60)$$

Having calculated B and knowing the Green's function, we determine $K_{1\bar{1}}^{11}$ from (45) and, after algebraic manipulations, we get a compact formula for the 2-point eigenvector correlation function from (34)

$$O_2(z_1, z_2) = \frac{1}{\pi} \partial_{\bar{z}_1} \partial_{z_2} \frac{\bar{z}_1(z_1 - z_2)O_1(r_1) + z_2(\bar{z}_1 - \bar{z}_2)O_1(r_2)}{|z_1 - z_2|^2 [F(r_1) - F(r_2)]}. \quad (61)$$

The quaternionic R-transform of biunitarily invariant ensembles takes a remarkably simple form [47], in particular $R_{1\bar{1}}(Q) = Q_{1\bar{1}}A(Q_{1\bar{1}}Q_{\bar{1}1})$. Moreover, due to the rotational symmetry of the spectrum, $\mathfrak{g}(z) = 1/z$. According to (48), the traced product of resolvents is given by

$$\mathfrak{h}(z_1, z_2) = \frac{1}{z_1 \bar{z}_2 - A(0)}. \quad (62)$$

Interestingly, $A(0) = r_{out}^2$, where r_{out} is the external radius of the spectrum. This result shows a high level of universality, since for any two function f, g analytic in the spectrum, in the $N \rightarrow \infty$ limit, the expectation

$$\left\langle \frac{1}{N} \text{Tr} f(X)g(X^\dagger) \right\rangle = \frac{1}{(2\pi i)^2} \int_{\gamma} dz_1 \int_{\bar{\gamma}} d\bar{z}_2 \frac{f(z_1)g(\bar{z}_2)}{z_1 \bar{z}_2 - r_{out}^2} \quad (63)$$

is given by the same formula, irrespectively on the specific biunitarily invariant ensemble. r_{out} can be set to 1 by rescaling of the matrix. This result, appearing naturally in the language of cumulants, from the point of the spectral decomposition, $X = \sum_k |R_k\rangle \lambda_k \langle L_k|$, is far from being obvious and may explain the simplicity of formula (61).

4 Examples

4.1 Elliptic Ensemble

As a first example of application of this formalism, we take the Elliptic Ensemble. Due to the fact that only the second cumulants do not vanish, the sum in (46) reduces to a single term and B is diagonal $B_{Ell} = \text{diag}(\sigma^2\tau, \sigma^2, \sigma^2, \sigma^2\tau)$. However, the equations (45) do not decouple, because the Green's functions are not diagonal in the non-holomorphic regime. Denoting for $j = 1, 2$

$$G_j = \begin{pmatrix} \frac{\bar{z}_j - z_j\tau}{\sigma^2(1-\tau^2)} & \frac{i}{\sigma^2} \sqrt{1 - \frac{|z_j - \bar{z}_j\tau|^2}{\sigma^2(1-\tau^2)}} \\ \frac{i}{\sigma^2} \sqrt{1 - \frac{|z_j - \bar{z}_j\tau|^2}{\sigma^2(1-\tau^2)}} & \frac{z_j - \bar{z}_j\tau}{\sigma^2(1-\tau^2)} \end{pmatrix} \quad (64)$$

the Green's function of the Elliptic Ensemble in the non-holomorphic regime (see Appendix A), we find K , solving (45)

$$K = (\mathbf{1} - (G_1 \otimes G_2^T)B_{Ell})^{-1} (G_1 \otimes G_2^T). \quad (65)$$

Then we focus on the component $K_{1\bar{1}}^{11}$ and differentiate it twice, according to (34), obtaining

$$O_2(z_1, z_2) = \frac{1}{\pi^2} \partial_{\bar{z}_1} \partial_{z_2} K_{1\bar{1}}^{11} = -\frac{\sigma^2(1-\tau^2)^2 - (z_1 - \bar{z}_2\tau)(\bar{z}_2 - z_1\tau)}{\pi^2 \sigma^2(1-\tau^2) |z_1 - z_2|^4}. \quad (66)$$

This result was derived for the first time by Chalker and Mehlig [10]². For the Ginibre Ensemble ($\sigma = 1, \tau = 0$) it reduces to

$$O(z_1, z_2) = \frac{-1}{\pi^2} \frac{1 - z_1 \bar{z}_2}{|z_1 - z_2|^4}. \quad (67)$$

For the completeness, we remark that the holomorphic part of the two point function, calculated from (48), reads

$$\mathfrak{h}(z_1, \bar{z}_2) = \frac{4}{-4 + (z_1 + \sqrt{z_1^2 - 4\sigma^2\tau})(\bar{z}_2 + \sqrt{\bar{z}_2^2 - 4\sigma^2\tau})}. \quad (68)$$

4.2 Biunitarily invariant ensembles

We consider some examples where the two-point function can be easily calculated. By no means this list is exhausted, in fact biunitary invariance is preserved under addition and multiplication, thus one can easily generate new ensembles. We do not present results for products of the ensembles below, only due to the fact that the expressions for $O_2(z_1, z_2)$ become lengthy.

- *Ginibre* As a cross-check of correctness of our formula, let us first consider the Ginibre ensemble. Its spectral density is uniform on the unit disk, therefore $F(r) = 2\pi \int_0^r s \frac{\theta(1-s)}{\pi} ds$ is equal to 1 for $r > 1$ and $F(r) = r^2$ for $r \leq 1$. Substitution to (61) reproduces the result derived earlier (67).
- *Induced Ginibre* [53] Let us consider a rectangular $N \times M$ matrix X (without loss of generality, $M > N$) with iid Gaussian entries. There exists an $M \times M$ unitary matrix U so that $Y = XU$ can be represented in the block form $Y = (X', 0)$. The right $N \times (M - N)$ block consists of zeros, while X' is called the induced Ginibre matrix. In the limit $N, M \rightarrow \infty$ with $\alpha = \frac{M-N}{N}$ fixed, its radial cdf reads

$$F(r) = \begin{cases} 0 & \text{for } r < \sqrt{\alpha} \\ r^2 - \alpha & \text{for } \sqrt{\alpha} < r < \sqrt{\alpha + 1} \\ 1 & \text{for } r > \sqrt{1 + \alpha} \end{cases} \quad (69)$$

Substitution into (61) after some algebra yields

$$O_{Ind}(z_1, z_2) = \frac{1}{\pi^2} \frac{(1 + \alpha - z_1 \bar{z}_2)(\alpha - z_1 \bar{z}_2)}{z_1 \bar{z}_2 |z_1 - z_2|^4}. \quad (70)$$

The Ginibre Ensemble corresponds to $\alpha = 0$.

- *Truncated Unitary* [54] Let us consider a $(N + L) \times (N + L)$ random unitary matrix the pdf of which is given by the Haar measure on $U(N + L)$ and remove its last L rows and column. The radial cdf of the remaining square matrix in the limit $N, L \rightarrow \infty$ with $\kappa = \frac{L}{N}$ fixed reads $F(r) = \kappa \frac{r^2}{1 - r^2}$ for $r < (1 + \kappa)^{-1/2}$ and 1 otherwise [55]. Therefore the two-point eigenvector function reads

$$O_{TU}(z_1, z_2) = \frac{1}{\pi^2} \frac{-1 + z_1 \bar{z}_2 (1 + \kappa)}{|z_1 - z_2|^4}. \quad (71)$$

- *Spherical Ensemble* Consider a product $Y = X_1 X_2^{-1}$, where X_1 and X_2 are Ginibre matrices. Its radial cdf reads $F(r) = \frac{r^2}{1 + r^2}$ and its spectrum is unbounded [56]. This ensemble is beyond the assumptions made for derivation of (61). Nevertheless, motivated by the successful application of these methods for the one-point correlation function in this ensemble [29], we assume correctness of our formulas and calculate the two-point function

$$O_{Sph}(z_1, z_2) = \frac{1}{\pi^2} \frac{-1}{|z_1 - z_2|^4}. \quad (72)$$

- *Product of two Ginibre* We consider a matrix $Y = X_1 X_2$, where X_1 and X_2 are Ginibre matrices. The radial cdf of Y is $F(r) = \min(r, 1)$, thus

$$O_{prod}(z_1, z_2) = -\frac{1}{\pi^2} \frac{2(|z_1| + |z_2|)(z_1 \bar{z}_2 + |z_1 z_2|) - |z_1 + z_2|^2 - 4|z_1 z_2|}{4|z_1 z_2| |z_1 - z_2|^4}. \quad (73)$$

²[10, Eq.(94)] contains a small misprint in the constant factor, which does not affect validity of any other results therein.

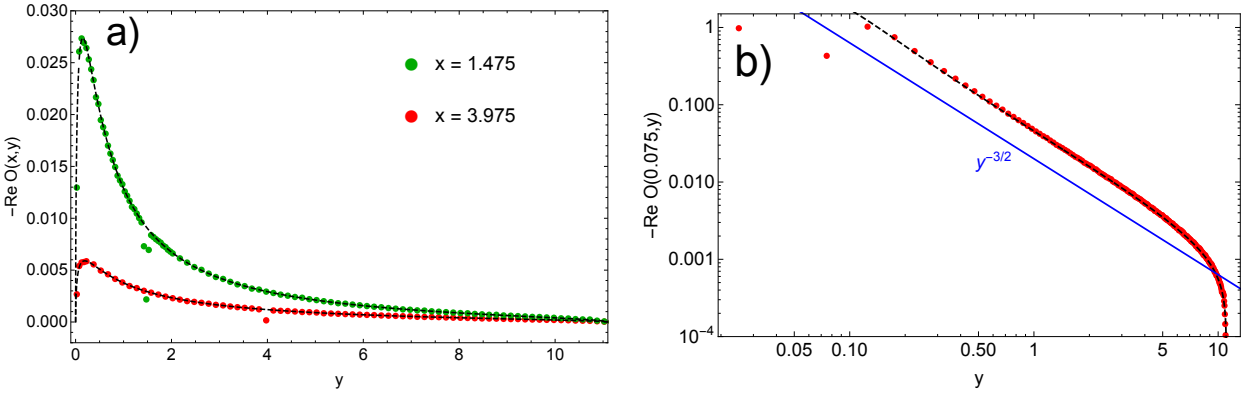


Figure 5: Cross sections of the two point eigenvector correlation function $O_2(x, y)$ for a) $x = 1.475, 3.975$ and b) $x = 0.075$. The numerical data (points) are obtained by diagonalization of $5 \cdot 10^4$ matrices of size $N = 100$. Black dashed lines are the solutions of (78) inserted into (37). Interestingly, if one of the arguments is close to the exceptional point $x = 0$, the large part of the function can be approximated by a power-law.

4.3 Pseudohermitian matrix

Let us consider a product $X = AB$ of two Hermitian matrices A, B . It is now not Hermitian, $X^\dagger = BA \neq X$, but if one of the matrices, let us say A , is positive definite, X is isospectral to a Hermitian matrix $A^{1/2}BA^{1/2}$, thus X , despite its non-Hermiticity, has real spectrum. The diagonalising matrix is, however, not unitary, resulting in non-orthogonality of eigenvectors. Such matrices can be toy-models for more complicated physical system described by Hamiltonians which are not Hermitian but possesses parity-time (PT) symmetry [57]. The most interesting models have a parameter which controls how far from the breaking of the symmetry the system is. At the critical value, called the exceptional point, two real eigenvalues coalesce and move away in the imaginary direction, spontaneously breaking the PT-symmetry.

As an example we consider a matrix $X = (2 + G_1)(2 + G_2)$, where G_i 's are independent matrices drawn from Gaussian Unitary Ensemble, the spectral density of which in the large N limit is the Wigner semicircle, $\rho_{\text{GUE}}(x) = \frac{1}{2\pi} \sqrt{4 - x^2}$, supported on the interval $[-2, 2]$. This model has an exceptional point at $x = 0$.

The components of the quaternionic R -transform of X read [58]

$$R_{11} = \frac{4(1 - G_{1\bar{1}}G_{\bar{1}1})(1 - G_{\bar{1}\bar{1}})^2}{(1 + G_{1\bar{1}}G_{\bar{1}1}(G_{\bar{1}\bar{1}} - 2) - G_{\bar{1}\bar{1}} + G_{11}(G_{\bar{1}\bar{1}} + G_{1\bar{1}}G_{\bar{1}1} - 1))^2}, \quad (74)$$

$$R_{1\bar{1}} = -\frac{G_{1\bar{1}}[-3 - G_{1\bar{1}}G_{\bar{1}1}(G_{\bar{1}\bar{1}} - 1) + G_{\bar{1}\bar{1}} + G_{11}(1 - G_{1\bar{1}}G_{\bar{1}1} + G_{\bar{1}\bar{1}})]^2}{(G_{1\bar{1}}G_{\bar{1}1} - 1)[1 + G_{1\bar{1}}G_{\bar{1}1}(G_{\bar{1}\bar{1}} - 2) - G_{\bar{1}\bar{1}} + G_{11}(G_{\bar{1}\bar{1}} - 1 + G_{1\bar{1}}G_{\bar{1}1})]^2}. \quad (75)$$

The other two components are given by the exchange of indices $1 \leftrightarrow \bar{1}$. Inserting it into (30) and focusing only on the holomorphic solution ($|w| = 0$), we arrive at the equation for the Green's function

$$\frac{4}{(1 - \mathbf{g}(z))^2} + \frac{1}{\mathbf{g}(z)} = z. \quad (76)$$

We choose a branch which gives the asymptotic behavior $\mathbf{g}(z) \sim 1/z$ for large z . The spectrum is supported on a single interval $[0, z_+]$, with $z_+ = \frac{1}{2}(11 + 5\sqrt{5})$. The Green's function infinitely close to the spectrum reads

$$\lim_{\epsilon \rightarrow 0} \mathbf{g}(x \pm i\epsilon) = \frac{1 + 2x}{3x} - \frac{1}{6x} \left(\frac{a}{r^{1/3}} (1 \pm i\sqrt{3}) - r^{1/3} (1 \mp i\sqrt{3}) \right), \quad (77)$$

where $a = 1 + 10x + x^2$ and $r = 1 + 15x + 39x^2 - z^3 - 6\sqrt{3}x\sqrt{x + 11x^2 - x^3}$. The imaginary part of the Green's function yields the spectral density, calculated in [59]. The traced product of resolvents according to (48) satisfies the equation

$$\frac{1}{\mathbf{h}(z_1, \bar{z}_2)} = \frac{1}{\mathbf{g}(z_1)\bar{\mathbf{g}}(\bar{z}_2)} - \frac{(1 - \mathbf{g}(z_1))^2(1 - \bar{\mathbf{g}}(\bar{z}_2))^2}{[-3 + \mathbf{g}(\bar{z}_2) + \mathbf{g}(z_1) + \mathbf{g}(z_1)\bar{\mathbf{g}}(\bar{z}_2)]^2}, \quad (78)$$

where $\mathbf{g}(z_1)$ and $\mathbf{g}(\bar{z}_2)$ are the solutions of (76) with the $1/z$ asymptotic behavior.

The two-point function is calculated from (36) and its cross-sections are juxtaposed with the numerical simulations in Fig. 5, showing an excellent agreement.

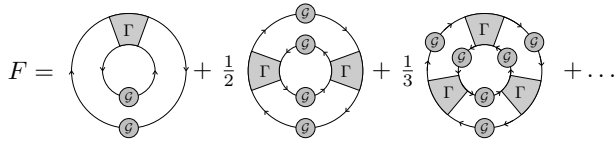


Figure 6: Hierarchy of wheel diagrams contributing to the two-point double-trace correlation function (80), which in turn correspond to the first possibility of contraction indices in Fig. 1. The combinatorial factor $1/n$ corresponds to rotational symmetry and prevents overcounting the diagrams.

5 Towards microscopic universality of eigenvectors

Random matrices show the phenomenon of universality at certain regions of the spectra. In the case of Hermitian ensembles, such universalities appear in the bulk (the so-called sine kernel) and at the edges of the spectra (Airy, Bessel, Pearcey, etc.) For a given generic Hermitian ensemble represented by N by N matrices H , one of the tools for investigating the existence of universalities are the multi-trace correlation functions

$$G(z_1, z_2, \dots, z_j) = \sum_{k_1, \dots, k_j=1}^{\infty} N^{j-2} \frac{\langle \text{tr} H^{k_1} \dots \text{tr} H^{k_j} \rangle_c}{z_1^{k_1+1} \dots z_k^{k_j+1}}. \quad (79)$$

The subscript c denotes the connected part.

Such objects were studied extensively using various techniques including loop equations [60], Coulomb gas analogy [61] and Feynman diagrams [45, 46]. They were put into a formal mathematical formulation of the higher order freeness [62, 63, 64]. When the eigenvalues occupy a single interval, they obey the Ambjorn-Jurkiewicz-Makeenko universality [60]. The divergences of the double-trace correlation function signal the breakdown of the $1/N$ expansion and the need of the resummation of the whole series accompanied with the rescaling of its arguments. Different universal limits are manifested as different types of singularities.

A natural generalization of the two-point double-trace function to the non-Hermitian setting is the connected average of two copies of the electrostatic potential (13)

$$F(Q, P) = \left\langle \frac{1}{N} \ln \det(\mathcal{Q} - \mathcal{X}) \frac{1}{N} \ln \det(\mathcal{P} - \mathcal{X}) \right\rangle_c, \quad (80)$$

introduced in [65], where also Gaussian models were considered. As the quaternionic Green's function, encoding all expectations of the traces can be obtained from the potential (see (18)), the function above generates all covariances of traces

$$\left\langle \frac{1}{N} \text{Tr} X^{\alpha_1} X^{\alpha_2} \dots X^{\alpha_k} \frac{1}{N} \text{Tr} X^{\beta_1} X^{\beta_2} \dots X^{\beta_l} \right\rangle_c, \quad (81)$$

being a natural extension of the second order freeness for large non-Hermitian matrices. Here $\alpha_i, \beta_j \in \{1, \dagger\}$.

As we mentioned earlier, the indices in the product of resolvent can be contracted in two ways, see Fig. 1. One of them gives access to the eigenvector correlation function, while the second one yields F . More precisely, $F(Q, P) = \text{Tr} L$. We shall not present the detailed derivation, we just mention that the diagrams contributing to F in the leading order are of wheel type [45, 46]. Their summation, presented in Fig. 6 yields

$$N^2 F(Q, P) = -\log \det [\mathbf{1} - (G(Q) \otimes G^T(P)) B(Q, P)]. \quad (82)$$

This means that the result, derived in [65] and used for deducing the existence of the edge universality [66], hold for the entire class of non-Hermitian models.

The two-point single-trace correlation functions encoding correlations between eigenvectors have also their counterpart in the Hermitian case, but because of reality of the spectrum and orthogonality of eigenvectors it trivially reduces to a one-point Green's function

$$\left\langle \frac{1}{N} \text{Tr} (z_1 \mathbf{1} - H)^{-1} (z_2 \mathbf{1} - H)^{-1} \right\rangle = \frac{\mathbf{g}(z_1) - \mathbf{g}(z_2)}{z_2 - z_1}, \quad (83)$$

therefore has not attracted attention. Eigenvectors of non-normal matrices are no longer trivial, making such correlation functions meaningful quantities.

In the guise of the above analysis, one is tempted to ask, if we can probe hypothetical *eigenvector universality* using similar tools. We would like to stress, that even in the case of the simplest Ginibre ensemble, the direct analysis of the eigenvector correlation functions is very hard. Whereas the finite N expression for one point

function is known [10, 23], the only known non-perturbative results for the calculation of the 2-point eigenvector correlation function are given implicitly [9, 10]

$$O_2(z_1, z_2) = -\frac{N}{\pi^2 \Gamma(N)} e^{-N(|z_1|^2 + |z_2|^2)} \det [h_{ij}]_{i,j=0}^{N-2}, \quad (84)$$

where the matrix h is pentadiagonal with entries given by

$$h_{ij} = \frac{N^{j+3}}{\pi(j+1)!} \int d^2 \lambda \bar{\lambda}^i \lambda^j \left[|z_1 - \lambda|^2 |z_2 - \lambda|^2 + \frac{1}{N} (z_1 - \lambda)(\bar{z}_2 - \bar{\lambda}) \right] e^{-N|\lambda|^2}. \quad (85)$$

There is, however, a different possibility of inferring the existence of universality. Spectra of non-normal matrices are intimately linked with the properties of their eigenvectors. The completeness relation $\sum_{k=1}^N |R_k\rangle \langle L_k| = 1$ used in the weighted density (3) leads to the sum rule $\int_{\mathbb{C}} d\mu(w) D(z, w) = \rho(z)$, which imposes constraints on the eigenvector correlation functions

$$N O_1(z) + \int_{\mathbb{C}} d\mu(w) O_2(z, w) = \rho(z). \quad (86)$$

While the right hand side is of order 1, the one-point correlator gives a contribution of order N , thus there has to be a counterterm from the integral. As the region of integration is in fact compact in the large N limit, the divergence can stem only from the region when w is close to z . The exact calculations in this regime are not accessible within the diagrammatic approach, but below we give a qualitative argument that the microscopic scaling is responsible for cancellation of divergences.

In RMT the microscopic universality can be probed on the scale of the typical distance between eigenvalues. A standard argument that in the disk of radius δz centered at z we should expect of the order of one eigenvalue leads to the scaling

$$w = z + \frac{u}{\sqrt{N\rho(z)}}, \quad (87)$$

where $u \sim 1$. We notice that in all examples presented in Sec. 4 the two-point function can be expressed as

$$O_2(z, w) = -\frac{1}{\pi^2} \frac{P(z, w)}{|z - w|^4} \quad (88)$$

with the same behavior in the denominator. The microscoping scaling (87) inserted in the denominator produces a term $(N\rho(z))^2$, while the Jacobian of the change of variables reduces the power to one, giving the desired behavior in N . Moreover, by explicit evaluation of derivatives in (61) and application of de l'Hospital's rule twice we get for biunitarily invariant ensembles $P(z, z) = \frac{O(z)}{\rho(z)}$, which cancels densities, eventually leaving only the one-point function, which produce the desired counterterm. We hypothesize that this phenomenon is universal across all non-Hermitian ensembles in the bulk.

Motivated by the ubiquitousness of the $|z-w|^{-4}$ divergence in the bulk we state the conjecture that in generic non-Hermitian matrices for all points in the bulk at which the spectral density does not develop singularities there exists a microscoping limit

$$\lim_{N \rightarrow \infty} N^{-2} O(z + \frac{x}{\sqrt{N}}, z + \frac{y}{\sqrt{N}}) = O_1(z) \Phi(|x - y|), \quad (89)$$

where

$$\Phi(|\omega|) = -\frac{1}{\pi^2 |\omega|^4} \left(1 - (1 + |\omega|^2) e^{-|\omega|^2} \right). \quad (90)$$

The function Φ was calculated in [9, 10] by evaluation of $O(0, z)$ from the exact result (84) and taking the scaling limit $z = \frac{\omega}{\sqrt{N}}$. It is presented in Fig. 7a) and compared with the evaluation of the exact formula.

Interestingly, performing analogous reasoning for Ginibre ensemble (in which $P(z, w) = 1 - z\bar{w}$) when z is at the edge of the spectrum leads us to a different conclusion. When two arguments get close, the two-point function diverges, but as $|z - w|^{-3}$, because P also vanishes, reducing the exponent. This suggests that at the edge the two-point function scales as $N^{3/2}$ instead of N^2 in the bulk. This stays in agreement with the sum rule (86), since O_1 at the edge scales as $N^{1/2}$ [23]. The limiting scaling function is not available to us, we evaluate numerically (84) and show the results in Fig. 7b). The divergence of the two-point function at the origin for the product of two Ginibre matrices (73) also suggests the existence of a different scaling there.

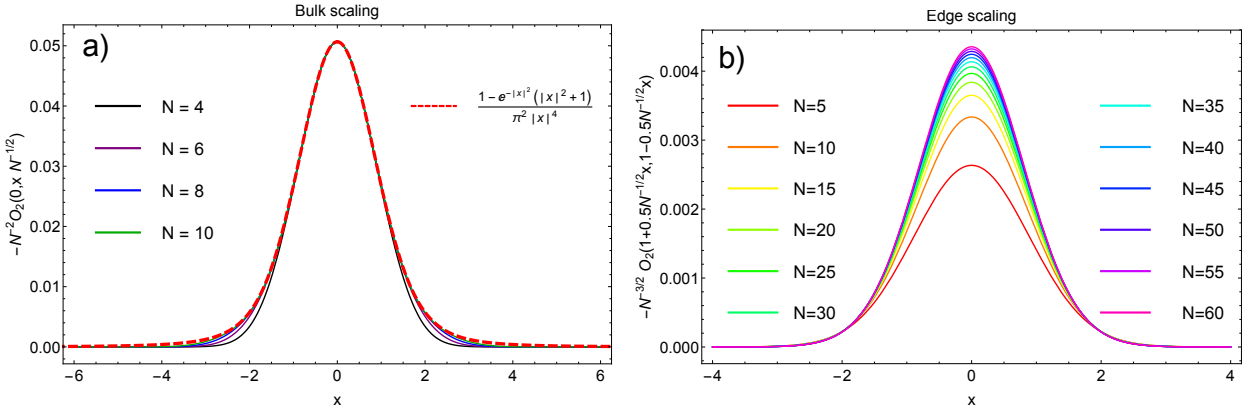


Figure 7: The two-point eigenvector correlation function $O_2(z_1, z_2)$ for the Ginibre ensemble in the microscopic a) bulk regime, $z_1 = 0$, $z_2 = \frac{x}{\sqrt{N}}$ and b) edge regime $z_1 = 1 + \frac{x}{2\sqrt{N}}$, $z_2 = 1 - \frac{x}{2\sqrt{N}}$. Red dashed line is the Chalker and Mehlig's exact result (90). In the bulk microscopic regime O_2 scales as N^2 , while at the edge with $N^{3/2}$. The rapid convergence to the limiting bulk scaling suggest that the corrections are exponentially small, while the hypothetical edge scaling seems to have $1/N$ corrections.

6 Summary

Using the methods of the quaternion formalism [67] for the non-Hermitian random matrices, we have proposed the explicit calculational scheme for the two-point eigenvector correlation function (4). First, we have checked that our formalism reproduces all known examples in the literature, i.e. complex Ginibre ensemble, an elliptic ensemble and open chaotic scattering ensemble. Second, we considered two subclasses of non-normal random matrices: the pseudohermitian and the biunitarily invariant ensembles, which in the large N limit are described by the R -diagonal operators from free probability [68, 69]. In both cases we got new results for the two-point eigenvector correlation functions. In the case of the bi-unitarily invariant ensembles, the two-point function $O_2(z, w)$ has particularly simple form. It is expressed solely as a function of the radial cumulative distribution function $F(r)$ and the one-point eigenvector correlation function $O_1(r)$.

Recently, it was proven [29] that for biunitarily invariant ensembles, $O_1(r)$ can be expressed in terms of $F(r)$ exclusively, which can be viewed as an extension of the single ring (Haagerup-Larsen) theorem [48, 50]. Combining this result with our formalism, we arrive at the conclusion, that the two-point eigenvector correlation function for general biunitarily invariant ensembles in the large N limit depends functionally solely on the spectral density. Such a situation resembles the Ambjorn-Jurkiewicz-Makeenko (known also as Brezin-Zee) universality in the case of Hermitian random matrix models, where the two-point spectral Green's function depends solely on the one-point Green's function, irrespectively on the specific ensemble. Mathematical formulation of such a construction is known as the second order freeness [62]. We are therefore tempted to speculate, that, by combining second order freeness and freeness with amalgamation [70], the notion of the non-orthogonality of eigenvectors can be extended into a broader context of operators in von Neumann algebras. Indeed, a similar equation to (45) has recently appeared in the description of fluctuations of Gaussian block matrices [71].

The similarity of our result to AJM (BZ) universality has further consequences. In the case of the ABJ (BZ) universality, the singular points of the correlation functions identify the regions of the spectra, where microscopic universality takes place. This includes both the cases of the bulk and edge universality. We are therefore inclined to apply similar argument for our result, searching for the microscopic eigenvector universalities. An additional argument for the microscopic universality comes from the constraint on eigenvector correlation function (86), as originally noted by Walters and Starr. The sum rules, originating from this constraint, strongly suggest the universal form of the microscopic two-point eigenvector correlations, in analogy to similar phenomenon for sum rules of Dirac Euclidean operators, found by Leutwyler and Smilga [72], which lead Stony Brook group to the discovery of the universal Bessel kernels for chiral random matrix models [73, 74].

Our analysis, as well as explicit examples for the bi-unitarily invariant ensembles calculated in Sec. 4.2, point at the generic shape of such universality, coming from the ubiquitous factor in denominator $|z - w|^4$. Explicitly, $O_2(z, w) = -\frac{1}{\pi^2} \frac{P(z, w)}{|z - w|^4}$, where $\lim_{z \rightarrow w} P(z, w) = O_1(z)/\rho(z)$ yields the Petermann factor. Such unique behavior is responsible for the crucial cancellation of the divergent terms in the leading order in N in the sum rules. Identification of this mechanism leads us to the prediction of the existence of the universal microscopic scaling of the eigenvector correlation function $\Phi(|\omega|)$. Such limit was obtained in the special case of the Ginibre ensemble [9, 10]. We conjecture that this universality extends to at least biunitarily invariant random ensembles.

Interestingly, the sum rule (86) lead also to the interesting predictions at the edge. It is well known, that

correlations of eigenvalues of non-Hermitian matrices exhibit universal behavior at the edge, given by the error function. Our large N results for the eigenvector correlations show, that at the edge the leading singularity weakens, $|z - w|^4 \rightarrow |z - w|^3$, leading to $N^{3/2}$ scaling of two-point correlation function. Numerical evaluation of the implicit exact result (84) confirms this hypothesis, but the analytic form of the scaling function is not yet available, even in the case of the simplest, complex Ginibre ensemble.

Our results are only one of the step towards understanding of the statistical properties of non-normal random operators and give rise to new questions. The matrix of overlaps O_{ij} is the simplest invariant object. It is natural to ask what kind of non-trivial higher order invariants can be built out of eigenvector. This problem is even more cumbersome in the light of the recent results [24, 33], because the distribution of the diagonal overlap O_{ii} is heavy tailed and some objects, like for instance $\langle O_{ii}^2 \rangle$, do not exist. For the real Ginibre ensemble the situation is even more hopeless, since at the real axis the one-point function O_1 does not exist! While one expects existence of certain correlation function involving local averages of *distinct* eigenvectors, it is unclear whether their mathematical structure simplifies as it is for spectral statistics, which form determinantal point processes. Even though, due to the eigenvalue repulsion, an event that two or more eigenvalues lie close to each other is unlikely to happen, correlations between their eigenvectors do not decay, as can be seen from the microscopic scaling of O_2 . It is therefore very appealing to study microscopic eigenvector correlations involving more than two eigenvalues.

The issue of hypothetical microscopic eigenvector universality for generic non-Hermitian ensembles is also of primary importance, since unraveling the unknown microscopic eigenvector correlations may give hope in the case of notorious sign problems by giving an insight into the properties of the Dirac operator in Euclidean QCD at non-zero chemical potential.

Note added. After completing this manuscript, we became aware of a recent work by Bourgade and Dubach [24], which tackles the issue of eigenvector correlations in the complex Ginibre ensemble in the bulk using different probabilistic techniques. They found the full probability of the diagonal overlap as an inverse gamma distribution and also studied first two moments of the off-diagonal overlap. Moreover they proved that the result for the macroscopic two-point function (67) extends to mesoscopic scales.

Acknowledgements

WT appreciates the financial support from the Polish Ministry of Science and Higher Education through ‘Diamond Grant’ 0225/DIA/2015/44 and the scholarship of Marian Smoluchowski Research Consortium Matter Energy Future from KNOW funding. The authors thank Piotr Warchał for discussions. The authors are grateful to Paul Bourgade for correspondence and useful remarks.

Appendix A One point functions in Elliptic Ensemble

It is very instructive to show how the formalism described in Sec. 2 works in practice. Let us consider a non-Hermitian matrix model given by the Gaussian potential (21). Due to the fact that there are no vertices in this model, the only cumulants are $c_{\alpha\beta}^{(2)}$, given by the propagators. This completely determines the quaternionic R -transform

$$R(Q) = \sigma^2 \begin{pmatrix} \tau Q_{11} & Q_{1\bar{1}} \\ Q_{\bar{1}1} & \tau Q_{\bar{1}\bar{1}} \end{pmatrix}. \quad (91)$$

Once we performed the average over the ensemble (i.e. we know the form of R), we can safely remove the regularization, by setting $|w| = 0$ at the level of the algebraic equation (30), which in this case reads

$$\sigma^2 \begin{pmatrix} \tau G_{11} & G_{1\bar{1}} \\ G_{\bar{1}1} & \tau G_{\bar{1}\bar{1}} \end{pmatrix} + \frac{1}{G_{11}G_{\bar{1}\bar{1}} - G_{1\bar{1}}G_{\bar{1}1}} \begin{pmatrix} G_{\bar{1}\bar{1}} & -G_{1\bar{1}} \\ -G_{\bar{1}1} & G_{11} \end{pmatrix} = \begin{pmatrix} z & 0 \\ 0 & \bar{z} \end{pmatrix}. \quad (92)$$

Focusing on the $1\bar{1}$ component, one gets

$$G_{1\bar{1}} \left(\sigma^2 - \frac{1}{G_{11}G_{\bar{1}\bar{1}} - G_{1\bar{1}}G_{\bar{1}1}} \right) = 0. \quad (93)$$

There are two solutions, a trivial one $G_{1\bar{1}} = 0$ and a non-trivial $\sigma^2 = (G_{11}G_{\bar{1}\bar{1}} - G_{1\bar{1}}G_{\bar{1}1})^{-1}$. Let us focus on the trivial first. Inserting $G_{1\bar{1}} = 0$ into the equation given by the 11 component, we get $\sigma^2\tau G_{11} + 1/G_{11} = z$, with two solutions

$$G_{11}(z) = \frac{z \pm \sqrt{z^2 - 4\sigma^2\tau}}{2\sigma^2\tau} = \mathfrak{g}(z). \quad (94)$$

This is the holomorphic part, valid outside the spectrum and we have to choose the branch of the solution with a minus sign for a correct asymptotic behavior at infinity $\mathfrak{g}(z) \sim 1/z$. In the holomorphic domain, the

off-diagonal elements of the Green's function vanish, because the one-point eigenvector correlation function is trivially zero as there are no eigenvalues there.

Considering the non-trivial solution of (93) and inserting it to the equations for 11 and $\bar{1}\bar{1}$ components, we obtain a system of two linear equations

$$\begin{aligned}\sigma^2\tau G_{11} + \sigma^2 G_{\bar{1}\bar{1}} &= z, \\ \sigma^2\tau G_{\bar{1}\bar{1}} + \sigma^2 G_{11} &= \bar{z},\end{aligned}$$

with the solution

$$G_{11}(z) = \frac{\bar{z} - z\tau}{\sigma^2(1 - \tau^2)}. \quad (95)$$

The spectral density is calculated according to (11):

$$\rho(z, \bar{z}) = \frac{1}{\pi} \partial_{\bar{z}} G_{11} = \frac{1}{\pi\sigma^2(1 - \tau^2)}. \quad (96)$$

One can also calculate $G_{1\bar{1}}$ and get the following formula for the one-point eigenvector correlation function from (17)

$$O_1(z) = \frac{1}{\pi\sigma^2} \left(1 - \frac{|z - \bar{z}\tau|^2}{\sigma^2(1 - \tau^2)^2} \right). \quad (97)$$

The boundary of the spectrum can be calculated in two ways: by imposing the matching of the holomorphic and non-holomorphic solutions at the boundary or by imposing vanishing of the one-point eigenvector correlation function. Both methods give

$$\frac{x^2}{(1 + \tau)^2} + \frac{y^2}{(1 - \tau)^2} = \sigma^2, \quad (98)$$

which is the equation for the ellipse with semi-axes $\sigma(1 + \tau)$ and $\sigma(1 - \tau)$, hence the name of the ensemble.

Appendix B Quantum scattering ensemble

Let us see how the procedure for determining the rung of the ladder works in practice. We consider the quantum scattering ensemble [75] given by

$$X = H + i\gamma\Gamma, \quad (99)$$

where H is $N \times N$ complex matrix with Gaussian entries of zero mean and variance $\langle |H_{kl}|^2 \rangle = N^{-1}\delta_{kl}$ and $\Gamma = \sum_{a=1}^M V^a (V^a)^\dagger$. The components of N -dimensional vectors V^a 's are complex Gaussians with variance $\langle V_k^a \bar{V}_l^b \rangle = N^{-1}\delta_{kl}\delta_{ab}$. In the limit $M, N \rightarrow \infty$ but with $M/N = m$ fixed (planar limit) the two point eigenvector correlation function was studied by Mehlig and Santer [34]. We show how this result can be derived within this formalism in a simpler way.

Γ is the complex Wishart matrix [76] multiplied by m . The planar cumulants of the Wishart matrix are stored in the Voiculescu's R-transform from free probability, which reads $R_\Gamma(z) = \frac{m}{1-z}$. The considered matrix X is non-Hermitian, therefore we need its quaternionic R-transform. Using the embedding of the complex R-transform into the quaternionic structure [67], we get $R_\Gamma(Q) = m(\mathbf{1}_2 - Q)^{-1}$. The Gaussian matrix is a particular instance of Elliptic Ensemble corresponding to $\tau = 1$, therefore $R_H(Q) = Q$. Further, Γ is rescaled by a complex number $i\gamma$. The quaternionic R-transform of such a rescaled matrix is obtained from the relation [67] $R_{i\gamma\Gamma}(Q) = gR_\Gamma(Qg)$, where $g = \text{diag}(i\gamma, -i\gamma)$. As the R-transform is additive under addition of two matrices, we have $R_X(Q) = Q + mg(\mathbf{1} - Qg)^{-1}$, which we then expand into a power series

$$R_X(Q) = Q + mg \sum_{k=0}^{\infty} (Qg)^k. \quad (100)$$

Then we perform the procedure with hitting derivatives and substitution of the argument, described in Sec 3.3. After summing up the resulting series, we get

$$B_{\mu\nu}^{\alpha\beta}(Q, P) = \delta^{\alpha\beta}\delta_{\nu\mu} + m (g^{-1} - G(Q))_{\alpha\beta}^{-1} (g^{-1} - G^T(P))_{\mu\nu}^{-1}. \quad (101)$$

This can be written in the matrix form as

$$B(Q, P) = \mathbf{1} + m [g^{-1} - G(Q)]^{-1} \otimes [g^{-1} - G^T(P)]^{-1}. \quad (102)$$

Inserting this into (45), we reproduce the results of [34]. The Green's function is calculated from (30).

References

- [1] Lloyd Nicholas Trefethen and Mark Embree. *Spectra and pseudospectra: the behavior of nonnormal matrices and operators*. Princeton University Press, 2005.
- [2] V. Ratushnaya and R. Samtaney. Non-modal stability analysis and transient growth in a magnetized vlasov plasma. *EPL (Europhysics Letters)*, 108(5):55001, 2014.
- [3] Saikiran Rapaka, Shiyi Chen, Rajesh J. Pawar, Philip H. Stauffer, and Dongxiao Zhang. Non-modal growth of perturbations in density-driven convection in porous media. *Journal of Fluid Mechanics*, 609:285–303, 2008.
- [4] Michael G. Neubert and Hal Caswell. Alternatives to resilience for measuring the responses of ecological systems to perturbations. *Ecology*, 78(3):653–665, 1997.
- [5] Malbor Asllani and Timoteo Carletti. Topological resilience in non-normal networked systems. *arXiv preprint arXiv:1706.02703*, 2017.
- [6] A. E. Siegman. Lasers without photons — or should it be lasers with too many photons? *Applied Physics B*, 60(2):247–257, Feb 1995.
- [7] Brian F. Farrell and Petros J. Ioannou. Stochastic dynamics of baroclinic waves. *Journal of the Atmospheric Sciences*, 50(24):4044–4057, 1993.
- [8] D. Borba, K. S. Riedel, W. Kerner, G. T. A. Huysmans, M. Ottaviani, and P. J. Schmid. The pseudospectrum of the resistive magnetohydrodynamics operator: Resolving the resistive alfvén paradox. *Physics of Plasmas*, 1(10):3151–3160, 1994.
- [9] JT Chalker and B Mehlig. Eigenvector statistics in non-hermitian random matrix ensembles. *Physical review letters*, 81(16):3367, 1998.
- [10] B Mehlig and JT Chalker. Statistical properties of eigenvectors in non-hermitian gaussian random matrix ensembles. *Journal of Mathematical Physics*, 41(5):3233–3256, 2000.
- [11] Romuald A. Janik, Wolfgang Nörenberg, Maciej A. Nowak, Gábor Papp, and Ismail Zahed. Correlations of eigenvectors for non-hermitian random-matrix models. *Phys. Rev. E*, 60:2699–2705, Sep 1999.
- [12] Brendan K. Murphy and Kenneth D. Miller. Balanced amplification: A new mechanism of selective amplification of neural activity patterns. *Neuron*, 61(4):635 – 648, 2009.
- [13] Guillaume Hennequin, Tim P. Vogels, and Wulfram Gerstner. Non-normal amplification in random balanced neuronal networks. *Phys. Rev. E*, 86:011909, Jul 2012.
- [14] Guillaume Hennequin, Tim P. Vogels, and Wulfram Gerstner. Optimal control of transient dynamics in balanced networks supports generation of complex movements. *Neuron*, 82(6):1394 – 1406, 2014.
- [15] Tommaso Biancalani, Farshid Jafarpour, and Nigel Goldenfeld. Giant amplification of noise in fluctuation-induced pattern formation. *Phys. Rev. Lett.*, 118:018101, Jan 2017.
- [16] L. Ridolfi, C. Camporeale, P. D’Odorico, and F. Laio. Transient growth induces unexpected deterministic spatial patterns in the turing process. *EPL (Europhysics Letters)*, 95(1):18003, 2011.
- [17] Václav Klika. Significance of non-normality-induced patterns: Transient growth versus asymptotic stability. *Chaos: An Interdisciplinary Journal of Nonlinear Science*, 27(7):073120, 2017.
- [18] Yan V. Fyodorov and Dmitry V. Savin. Statistics of resonance width shifts as a signature of eigenfunction nonorthogonality. *Phys. Rev. Lett.*, 108:184101, May 2012.
- [19] J.-B. Gros, U. Kuhl, O. Legrand, F. Mortessagne, E. Richalot, and D. V. Savin. Experimental width shift distribution: A test of nonorthogonality for local and global perturbations. *Phys. Rev. Lett.*, 113:224101, Nov 2014.
- [20] Ramis Movassagh. Eigenvalue attraction. *Journal of Statistical Physics*, 162(3):615–643, Feb 2016.
- [21] Zdzislaw Burda, Jacek Grela, Maciej A. Nowak, Wojciech Tarnowski, and Piotr Warchol. Dysonian dynamics of the ginibre ensemble. *Phys. Rev. Lett.*, 113:104102, Sep 2014.

[22] Zdzisław Burda, Jacek Grela, Maciej A. Nowak, Wojciech Tarnowski, and Piotr Warchał. Unveiling the significance of eigenvectors in diffusing non-hermitian matrices by identifying the underlying burgers dynamics. *Nuclear Physics B*, 897(Supplement C):421 – 447, 2015.

[23] Meg Walters and Shannon Starr. A note on mixed matrix moments for the complex ginibre ensemble. *Journal of Mathematical Physics*, 56(1):013301, 2015.

[24] Paul Bourgade and Guillaume Dubach. The distribution of overlaps between eigenvectors of ginibre matrices. *arXiv preprint arXiv:1801.01219*, 2018.

[25] K. M. Frahm, H. Schomerus, M. Patra, and C. W. J. Beenakker. Large petermann factor in chaotic cavities with many scattering channels. *EPL (Europhysics Letters)*, 49(1):48, 2000.

[26] H. Schomerus, K.M. Frahm, M. Patra, and C.W.J. Beenakker. Quantum limit of the laser line width in chaotic cavities and statistics of residues of scattering matrix poles. *Physica A: Statistical Mechanics and its Applications*, 278(3):469 – 496, 2000.

[27] M. Patra, H. Schomerus, and C. W. J. Beenakker. Quantum-limited linewidth of a chaotic laser cavity. *Phys. Rev. A*, 61:023810, Jan 2000.

[28] K. Petermann. Calculated spontaneous emission factor for double-heterostructure injection lasers with gain-induced waveguiding. *IEEE Journal of Quantum Electronics*, 15(7):566–570, Jul 1979.

[29] Serban Belinschi, Maciej A Nowak, Roland Speicher, and Wojciech Tarnowski. Squared eigenvalue condition numbers and eigenvector correlations from the single ring theorem. *Journal of Physics A: Mathematical and Theoretical*, 50(10):105204, 2017.

[30] James Hardy Wilkinson. *The algebraic eigenvalue problem*, volume 87. Clarendon Press Oxford, 1965.

[31] Yan V. Fyodorov and B. Mehlig. Statistics of resonances and nonorthogonal eigenfunctions in a model for single-channel chaotic scattering. *Phys. Rev. E*, 66:045202, Oct 2002.

[32] Zdzisław Burda, Bartłomiej J. Spisak, and Pierpaolo Vivo. Eigenvector statistics of the product of ginibre matrices. *Phys. Rev. E*, 95:022134, Feb 2017.

[33] Yan V Fyodorov. On statistics of bi-orthogonal eigenvectors in real and complex ginibre ensembles: combining partial schur decomposition with supersymmetry. *arXiv preprint arXiv:1710.04699*, 2017.

[34] B. Mehlig and M. Santer. Universal eigenvector statistics in a quantum scattering ensemble. *Phys. Rev. E*, 63:020105, Jan 2001.

[35] Nelson Dunford, Jacob T Schwartz, William G Bade, and Robert G Bartle. Linear operators. part i, general theory. 1957.

[36] Roger A Horn and Charles R Johnson. *Matrix analysis*. Cambridge university press, 1990.

[37] Laszlo Erdos, Torben Krüger, and David Renfrew. Power law decay for systems of randomly coupled differential equations. *arXiv preprint arXiv:1708.01546*, 2017.

[38] Romuald A. Janik, Maciej A. Nowak, Gábor Papp, and Ismail Zahed. Non-hermitian random matrix models. *Nuclear Physics B*, 501(3):603 – 642, 1997.

[39] Romuald A. Janik, Maciej A. Nowak, Gábor Papp, Jochen Wambach, and Ismail Zahed. Non-hermitian random matrix models: Free random variable approach. *Phys. Rev. E*, 55:4100–4106, Apr 1997.

[40] Joshua Feinberg and A. Zee. Non-hermitian random matrix theory: Method of hermitian reduction. *Nuclear Physics B*, 504(3):579 – 608, 1997.

[41] J. T. Chalker and Z. Jane Wang. Diffusion in a random velocity field: Spectral properties of a non-hermitian fokker-planck operator. *Phys. Rev. Lett.*, 79:1797–1800, Sep 1997.

[42] Arthur Cayley. A memoir on the theory of matrices. *Philosophical Transactions of the Royal Society of London*, 148:17–37, 1858.

[43] Yan V Fyodorov, Boris A Khoruzhenko, and Hans-Jürgen Sommers. Almost-hermitian random matrices: eigenvalue density in the complex plane. *Physics Letters A*, 226(1):46 – 52, 1997.

[44] Bertrand Eynard et al. Counting surfaces, 2016.

[45] E Brézin and A Zee. Universal relation between green functions in random matrix theory. *Nuclear Physics B*, 453(3):531–551, 1995.

[46] Jerzy Jurkiewicz, Grzegorz Łukaszewski, and Maciej A Nowak. Diagrammatic approach to fluctuations in the wishart ensemble. *Acta Physica Polonica B*, 39(4), 2008.

[47] Maciej A. Nowak and Wojciech Tarnowski. Complete diagrammatics of the single-ring theorem. *Phys. Rev. E*, 96:042149, Oct 2017.

[48] Joshua Feinberg and A. Zee. Non-gaussian non-hermitian random matrix theory: Phase transition and addition formalism. *Nuclear Physics B*, 501(3):643 – 669, 1997.

[49] Alice Guionnet, Manjunath Krishnapur, and Ofer Zeitouni. The single ring theorem. *Annals of Mathematics*, 174(2):1189–1217, 2011.

[50] Uffe Haagerup and Flemming Larsen. Brown’s spectral distribution measure for r-diagonal elements in finite von neumann algebras. *Journal of Functional Analysis*, 176(2):331 – 367, 2000.

[51] Mario Kieburg and Holger Kösters. Exact relation between singular value and eigenvalue statistics. *Random Matrices: Theory and Applications*, 5(04):1650015, 2016.

[52] Alexandru Nica and Roland Speicher. *r*-diagonal pairs-a common approach to haar unitaries and circular elements. *The Fields Institute Communications*, 12(149), 1996.

[53] Jonit Fischmann, Wojciech Bruzda, Boris A Khoruzhenko, Hans-Jürgen Sommers, and Karol Życzkowski. Induced ginibre ensemble of random matrices and quantum operations. *Journal of Physics A: Mathematical and Theoretical*, 45(7):075203, 2012.

[54] Karol Życzkowski and Hans-Jürgen Sommers. Truncations of random unitary matrices. *Journal of Physics A: Mathematical and General*, 33(10):2045, 2000.

[55] Z. Burda, M. A. Nowak, and A. Swiech. Spectral relations between products and powers of isotropic random matrices. *Phys. Rev. E*, 86:061137, Dec 2012.

[56] Uffe Haagerup and Hanne Schultz. Brown measures of unbounded operators affiliated with a finite von neumann algebra. *Mathematica Scandinavica*, pages 209–263, 2007.

[57] Carl M Bender. Making sense of non-hermitian hamiltonians. *Reports on Progress in Physics*, 70(6):947, 2007.

[58] M A Nowak and W Tarnowski. In preparation.

[59] P Warchol. Dynamics in random matrix theory - toy model with spectral phase transition, 2010. Master Thesis.

[60] J. Ambjørn, J. Jurkiewicz, and Yu.M. Makeenko. Multiloop correlators for two-dimensional quantum gravity. *Physics Letters B*, 251(4):517 – 524, 1990.

[61] Fabio Deelan Cunden and Pierpaolo Vivo. Universal covariance formula for linear statistics on random matrices. *Phys. Rev. Lett.*, 113:070202, Aug 2014.

[62] James A. Mingo and Roland Speicher. Second order freeness and fluctuations of random matrices: I. gaussian and wishart matrices and cyclic fock spaces. *Journal of Functional Analysis*, 235(1):226 – 270, 2006.

[63] James A. Mingo, Piotr Śniady, and Roland Speicher. Second order freeness and fluctuations of random matrices: II. unitary random matrices. *Advances in Mathematics*, 209(1):212 – 240, 2007.

[64] Benoit Collins, James A Mingo, Piotr Śniady, and Roland Speicher. Second order freeness and fluctuations of random matrices. iii. higher order freeness and free cumulants. *Doc. Math.*, 12:1–70, 2007.

[65] Romuald A Janik, Maciej A Nowak, Gabor Papp, and Ismail Zahed. Non-hermitian random matrix models. *Nuclear Physics B*, 501(3):603–642, 1997.

[66] Romuald A. Janik, Maciej A. Nowak, Gábor Papp, and Ismail Zahed. Macroscopic universality: Why qcd in matter is subtle. *Phys. Rev. Lett.*, 77:4876–4879, Dec 1996.

[67] Andrzej Jarosz and Maciej A Nowak. Random hermitian versus random non-hermitian operators—unexpected links. *Journal of Physics A: Mathematical and General*, 39(32):10107, 2006.

- [68] Alexandru Nica and Roland Speicher. *r*-diagonal pairs-a common approach to haar unitaries and circular elements. *Field Institute Communications*, 12:149, 1996.
- [69] Fumio Hiai and Dénes Petz. *The semicircle law, free random variables and entropy*. Number 77. American Mathematical Soc., 2006.
- [70] Dimitri Shlyakhtenko. Random gaussian band matrices and freeness with amalgamation. *International Mathematics Research Notices*, 1996(20):1013–1025, 1996.
- [71] Mario Diaz, James Mingo, and Serban Belinschi. On the global fluctuations of block gaussian matrices. *arXiv preprint arXiv:1711.07140*, 2017.
- [72] H. Leutwyler and A. Smilga. Spectrum of dirac operator and role of winding number in qcd. *Phys. Rev. D*, 46:5607–5632, Dec 1992.
- [73] E.V. Shuryak and J.J.M. Verbaarschot. Random matrix theory and spectral sum rules for the dirac operator in qcd. *Nuclear Physics A*, 560(1):306 – 320, 1993.
- [74] J. J. M. Verbaarschot and I. Zahed. Spectral density of the qcd dirac operator near zero virtuality. *Phys. Rev. Lett.*, 70:3852–3855, Jun 1993.
- [75] Fritz Haake, Felix Izrailev, Nils Lehmann, Dirk Saher, and Hans-Jürgen Sommers. Statistics of complex levels of random matrices for decaying systems. *Zeitschrift für Physik B Condensed Matter*, 88(3):359–370, Oct 1992.
- [76] Romuald A Janik and Maciej A Nowak. Wishart and anti-wishart random matrices. *Journal of Physics A: Mathematical and General*, 36(12):3629, 2003.